

Heck  
Farrar

# CATALYTIC AIR POLLUTION CONTROL

Second  
Edition



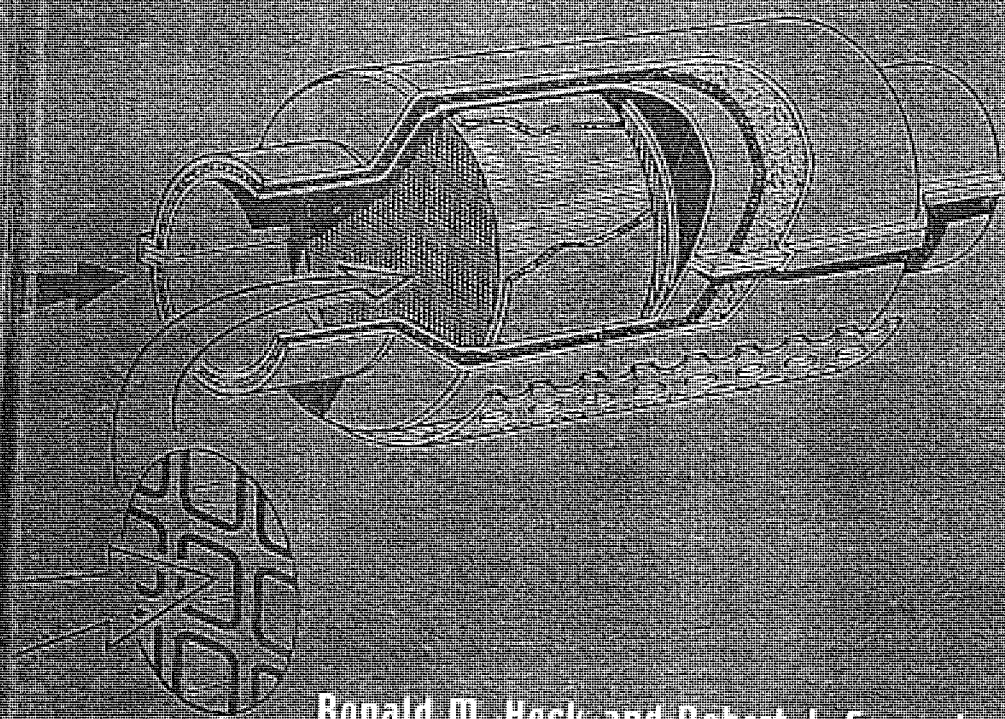
WILEY  
INTER-  
SCIENCE

BASF-2037.001

# CATALYTIC AIR POLLUTION CONTROL

*Commercial Technology*

Second Edition



Ronald M. Heck and Robert J. Farrauto  
with Suresh T. Gulati

BASF-2037.002

# **CATALYTIC AIR POLLUTION CONTROL**

**Second Edition**

**BASF-2037.003**



# CATALYTIC AIR POLLUTION CONTROL

Commercial Technology

---

Second Edition

Ronald M. Heck and Robert J. Farrauto  
with Suresh T. Gulati

 WILEY-  
INTERSCIENCE

A JOHN WILEY & SONS, INC., PUBLICATION

**BASF-2037.004**

This book is printed on acid-free paper. @

Copyright © 2002 by John Wiley & Sons, Inc., New York. All rights reserved.

Published simultaneously in Canada.

No part of this publication may be reproduced, stored in a retrieval system or transmitted in any form or by any means, electronic, mechanical, photocopying, recording, scanning or otherwise, except as permitted under Sections 107 or 108 of the 1976 United States Copyright Act, without either the prior written permission of the Publisher, or authorization through payment of the appropriate per-copy fee to the Copyright Clearance Center, 222 Rosewood Drive, Danvers, MA 01923, (978) 750-8400, fax (978) 750-4744. Requests to the Publisher for permission should be addressed to the Permissions Department, John Wiley & Sons, Inc., 605 Third Avenue, New York, NY 10158-0012, (212) 850-6011, fax (212) 850-6008, E-Mail: PERMREQ@WILEY.COM.

For ordering and customer service information please call 1-800-CALL-WILEY.

*Library of Congress Cataloging-in-Publication Data is available.*

ISBN 0-471-43624-0

Printed in the United States of America.

10 9 8 7 6

**BASF-2037.005**

To my wife, Barbara, whose friendship, support, understanding (especially on lost weekends), humor and selflessness made this endeavor much easier; Mercedes and Unk for always being there for support; and to Dutch who was overseeing it all.

*Ronald M. Heck*

To my wife Olga (Olechka) who has given me love, understanding, focus and a new vision of the wonders of life; my loving daughters Jill Marie and Maryellen and their husbands Glenn and Tom; special dedication to my beautiful grandchildren Nicky, Matthew, Kevin and Jillian and; God willing, their future brothers and sisters.

*Robert J. Farrauto*

To my wife Teresa whose encouragement and support helped make this possible; my sons Raj and Prem for their "you can do it, dad!" attitude; and my darling daughter Sonya for her "how can I help you, dad?" attitude throughout this project.

*Suresh T. Gulati*

# CONTENTS

PREFACE	xiii
ACKNOWLEDGMENTS	xvii
ACKNOWLEDGMENTS, FIRST EDITION	xix

I FUNDAMENTALS	1
----------------	---

1 Catalyst Fundamentals	3
-------------------------	---

- 1.1 The Basics: Activity and Selectivity 3
- 1.2 Dispersed Catalyst Model 5
- 1.3 The Steps in Heterogeneous Catalysis 6
- 1.4 The Arrhenius Equation 9
- 1.5 Significance of the Rate-Limiting Step 10

2 The Preparation of Catalytic Materials: Carriers, Active Components, and Monolithic Substrates	11
--	----

- 2.1 Introduction 11
- 2.2 Carriers 11
- 2.3 Making the Finished Catalyst 16
- 2.4 Nomenclature for Dispersed Catalysts 18
- 2.5 Monolithic Materials as Catalyst Substrates 18
- 2.6 Preparing Monolithic Catalysts 22
- 2.7 Catalytic Monoliths 23
- 2.8 Catalyzed Monolithic Nomenclature 23
- 2.9 Precious-Metal Recovery from Monolithic Catalysts 23

3 Catalyst Characterization	25
-----------------------------	----

- 3.1 Introduction 25
- 3.2 Physical Properties of Catalysts 26
- 3.3 Chemical Properties 34
- 3.4 Ex Situ Techniques 43

<b>4</b>	<b>Monolithic Reactors for Environmental Catalysis</b>	<b>45</b>
4.1	Introduction	45
4.2	Chemical Kinetic Control	45
4.3	Bulk Mass Transfer	47
4.4	Reactor Bed Pressure Drop	53
4.5	Summary	55
<b>5</b>	<b>Catalyst Deactivation</b>	<b>56</b>
5.1	Introduction	56
5.2	Thermally Induced Deactivation	56
5.3	Poisoning	61
5.4	Washcoat Loss	63
<b>II</b>	<b>MOBILE SOURCES</b>	<b>67</b>
<b>6</b>	<b>Automotive Catalyst</b>	<b>69</b>
6.1	Emissions and Regulations	69
6.2	The Catalytic Reactions for Pollution Abatement	72
6.3	The Physical Structure of the Catalytic Converter	73
6.4	First-Generation Converter: Oxidation Catalyst (1976–1979)	79
6.5	NO <sub>x</sub> , CO, and HC Reduction: The Second Generation (1979–1986)	83
6.6	Vehicle Test Procedure (U.S., Europe, and Japan)	88
6.7	NO <sub>x</sub> , CO, and HC Reduction: The Third Generation (1986–1992)	92
6.8	Palladium TWC Catalyst: The Fourth Generation (Mid-90s)	100
6.9	Low-Emission Catalyst Technologies	103
6.10	Modern TWC Technologies for the 2000s	110
6.11	Toward a Zero-Emission Stoichiometric Spark-Ignited Vehicle	112
6.12	Lean Burn Spark-Ignited Gasoline Engine	116
<b>7</b>	<b>Automotive Substrates</b>	<b>130</b>
7.1	Introduction to Ceramic Substrates	130
7.2	Requirements for Substrates	132
7.3	Design and Sizing of Substrates	134



15	7.4 Physical Properties of Substrates 139	
	7.5 Physical Durability 147	
	7.6 Advances in Substrate Development 160	
	7.7 Commercial Applications 171	
	7.8 Summary 178	
	7A Appendix 179	
6	<b>8 Diesel Engine Emissions</b>	<b>186</b>
	8.1 Introduction 186	
	8.2 Worldwide Diesel Emission Standards 188	
	8.3 NO <sub>x</sub> -Particulate Tradeoff 191	
	8.4 Analytic Procedures 192	
	8.5 Diesel Oxidation Catalyst for Treating SOF Portion of Particulates 192	
	8.6 Catalytic Reduction of Emissions from Diesel Passenger Cars 196	
	8.7 Catalyst Deactivation of the Diesel Oxidation Catalyst (DOC) 198	
	8.8 Treating Soot Using Diesel Particulate Filters (DPFs) 200	
	8.9 Dry Carbon Oxidation: Technologies under Development 202	
	8.10 NO <sub>x</sub> Reduction Technologies under Development 204	
	8.11 Natural-Gas Engines 208	
	<b>9 Diesel Catalyst Supports</b>	<b>212</b>
	9.1 Introduction 212	
	9.2 Diesel Oxidation Catalyst Supports 212	
	9.3 Design and Sizing of Diesel Filters 216	
	9.4 Regeneration Techniques 229	
	9.5 Physical Properties and Durability 235	
	9.6 Advances in Diesel Filters 240	
	9.7 Applications 249	
	9.8 Summary 259	
	<b>10 Ozone Abatement within Jet Aircraft</b>	<b>263</b>
	10.1 Introduction 263	
	10.2 Ozone Abatement 263	
	10.3 Deactivation 266	
	10.4 Analysis of In-flight Samples 269	
	10.5 New Technology 276	

### III STATIONARY SOURCES 279

#### 11 Volatile Organic Compounds 281

- 11.1 Introduction 281
- 11.2 Catalytic Incineration 282
- 11.3 Halogenated Hydrocarbons 285
- 11.4 Food Processing 291
- 11.5 Wood Stoves 295
- 11.6 Small Engines 295
- 11.7 Process Design 298
- 11.8 Deactivation 298
- 11.9 Regeneration of Poisoned Catalysts 298

#### 12 Reduction of NO<sub>x</sub> 306

- 12.1 Introduction 306
- 12.2 Nonselective Catalytic Reduction (NSCR) of NO<sub>x</sub> 306
- 12.3 Selective Catalytic Reduction (SCR) of NO<sub>x</sub> 310
- 12.4 Commercial Experience 318
- 12.5 Nitrous Oxide (N<sub>2</sub>O) 324
- 12.6 Catalytically Supported Thermal Combustion 324

#### 13 Carbon Monoxide and Hydrocarbon Abatement from Gas Turbines 334

- 13.1 Introduction 334
- 13.2 Catalyst for Carbon Monoxide Abatement 334
- 13.3 Nonmethane Hydrocarbon (NMHC) Removal 336
- 13.4 Oxidation of Reactive Hydrocarbons 338
- 13.5 Oxidation of Unreactive, Light Paraffins 339
- 13.6 Catalyst Deactivation 341

### IV EMERGING TECHNOLOGIES 345

#### 14 Fuel Cells 347

- 14.1 Introduction 347
- 14.2 Background 348
- 14.3 The Proton Exchange Membrane (PEM) Fuel Cell 351
- 14.4 Hydrogen Generation 355
- 14.5 Alkaline Fuel Cell 365
- 14.6 Phosphoric Acid Fuel Cell 366

CONTENTS xi

- 14.7 Molten Carbonate Fuel Cell 367
- 14.8 Solid Oxide Fuel Cell 369
- 14.9 Direct Methanol Fuel Cell 370
- 14.10 Commentary 371

15 Ambient Air Cleanup 376

- 15.1 Introduction 376
- 15.2 PremAir® Catalyst Systems 376
- 15.3 Other Approaches 384

INDEX 387

## 6 Automotive Catalyst

### 6.1 EMISSIONS AND REGULATIONS

The development of the spark-ignited combustion engine permitted the controlled combustion of gasoline that provides the power to operate the automobile. Gasoline, which contains a mixture of paraffins and aromatic hydrocarbons, is combusted with controlled amounts of air producing complete combustion products of  $\text{CO}_2$  and  $\text{H}_2\text{O}$



and also some incomplete combustion products of CO and unburned hydrocarbons (UHCs). The CO levels range from 1 to 2 vol%, while the unburned hydrocarbons range from 500 to 1000 vppm. During the combustion process very high temperatures are reached due to diffusion burning of the gasoline droplets, resulting in thermal fixation of the nitrogen in the air to form  $\text{NO}_x$  (Zeldovich 1946). Levels of  $\text{NO}_x$  are in the 100–3000 vppm ranges. The exhaust also contains approximately 0.3 moles of  $\text{H}_2$  per mole of CO. The quantity of pollutants varies with many of the operating conditions of the engine but is influenced predominantly by the air:fuel ratio in the combustion cylinder. Figure 6.1 shows the engine emissions from a spark-ignited gasoline engine as a function of the air:fuel ratio (Kummer 1980).

When the engine is operated rich of stoichiometric, the CO and HC emissions are highest while the  $\text{NO}_x$  emissions are depressed. This is because complete burning of the gasoline is prevented by the deficiency in  $\text{O}_2$ . The level of  $\text{NO}_x$  is reduced because the adiabatic flame temperature is reduced. On the lean side of stoichiometric, the CO and HC are reduced since nearly complete combustion dominates. Again, the  $\text{NO}_x$  is reduced since the operating temperature is decreased. Just lean of stoichiometric operation, the  $\text{NO}_x$  is a maximum, since the adiabatic flame temperature is the highest. At stoichiometric, the adiabatic flame temperature is lowered because of the heat of vaporization of the liquid fuel gasoline. The actual operating region of combustion for the spark-ignited engine is defined by the lean and rich flame stability, beyond which the combustion is too unstable (Searles 1989).

Within the region of operation of the spark-ignited engine, a significant amount of CO, HC, and  $\text{NO}_x$  is emitted to the atmosphere. The consequences of these emissions has been well documented (Viala 1993) but, briefly, CO is a

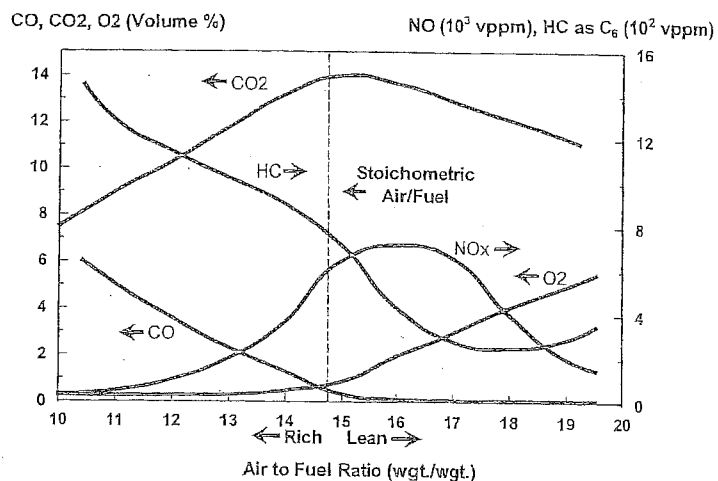


Figure 6.1 Spark-ignited gasoline engine emissions as a function of air:fuel ratio. [Copyright © 1980, reproduced with kind permission from Elsevier Sciences Lt (Kummer 1980).]

direct poison to humans, while HC and NO<sub>x</sub> undergo photochemical reaction in the sunlight leading to the generation of smog and ozone.

The need to control engine emissions was recognized as early as 1909 (Frankel 1909). The necessity to control automobile emissions in the United States came in 1970 when the U.S. Congress passed the Clean Air Act. The requirements under the Clean Air Act were changing as the technology was being evaluated. As a point of reference, the 1975/76 federal (49 states) requirements were 1.5 g/mi of HC, 15.0 g/mi of CO, and 3.1 g/mi of NO<sub>x</sub> (Hightower 1974). The Environmental Protection Agency (EPA) established the Federal Test Procedure (FTP) simulating the average driving conditions in the United States in which CO, HC, and NO<sub>x</sub> would be measured. The FTP cycle was conducted on a vehicle dynamometer and included measurements from the automobile during three conditions: (1) cold start, after the engine was idle for 8 h; (2) hot start, and (3) a combination of urban and highway driving conditions. Separate bags would collect the emissions from all three modes, and a weighing factor applied for calculating the total emissions. Complete details on the FTP test procedure are discussed later in this chapter. Typical precontrolled vehicle emissions in the total FTP cycle were 83–90 g/mi of CO, 13–16 g/mi of HC, and 3.5–7.0 g/mi of NO<sub>x</sub> (Hydrocarbon Processing 1971). A number of changes in engine design and control technology were implemented to lower the engine-out emissions; however, the catalyst was still required to obtain >90% conversion of CO and HC by 1976 and to maintain performance for 50,000 mi.

Amendments in the early 1990s to the Clean Air Act have set up more stringent requirements for automotive emissions (Calvert et al. 1993). The cat-

alysts will be required to last 100,000 mi for new automobiles after 1996. Further, these amendments (which were contingent on tier 2 standards to be set by EPAgency), reduce nonmethane hydrocarbon (NMHC) emissions to a maximum of 0.125 g/mi by 2004 (down from 0.41 g/mi in 1991), carbon monoxide to 1.7 g/mi (down from 3.4 g in 1991), and nitrogen oxides to 0.2 g/mi (down from 1.0 g). California in this same timeframe continued to set even more stringent regulations: NMHC emissions must be reduced to 0.075 g/mi by 2000 for 96% of all passenger cars. By 2003, 10% of these must have emissions no greater than 0.04 g/mi, and 10% must emit no NMHCs at all.

The current summary of the California emission standards for passenger cars is given below. LEV is the abbreviation for *low-emission vehicle*, while the T is transitional, U is ultra, and S is super; ZEV means zero-emission vehicle. The NMOG is nonmethane organics. As of 2000, the regulations are as follows:

Category	Durability Basis (miles)	NMOG (g/mile)	CO (g/mile)	NO <sub>x</sub> (g/mile)
TLEV	50,000	0.125	3.4	0.4
	120,000	0.156	4.2	0.6
LEV	50,000	0.075	3.4	0.05
	120,000	0.09	4.2	0.07
ULEV	50,000	0.04	1.7	0.05
	120,000	0.055	2.1	0.07
SULEV	120,000	0.010	1.0	0.02
ZEV	-0-	-0-	-0-	-0-

These are the most stringent worldwide vehicle emission regulations and will be the targets for all the worldwide manufacturers.

In comparison, the European standards for light duty gasoline engine passenger is as follows

Category	Stage 3 (2000)	Stage 4 (2005)
CO	2.3 g/km	1.0 g/km
UHC	0.2 g/km	0.1 g/km
NO <sub>x</sub>	0.15 g/km	0.08 g/km

The conversion factor from g/km to g/mile is 0.62.

Engine manufacturers have explored a wide variety of technologies to meet the requirements of the Clean Air Act. Catalysis has proved to be the most effective passive system. Presently the major worldwide suppliers of automotive catalysts are Engelhard, Johnson Matthey, DMC<sup>2</sup>, and Delphi. As the automobile engine has become more sophisticated, the control devices and combustion modifications have proved to be very compatible with catalyst tech-



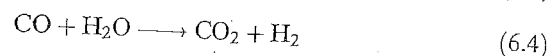
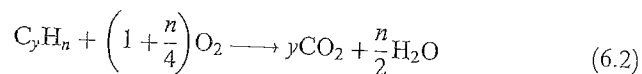
nology, to the point where today engineering design incorporates the emission control unit and strategy for each vehicle. The ZEV vehicles will probably be battery-operated. California Air Resources Board (CARB) is also implementing the PZEV vehicle, which is basically a SULEV vehicle with zero evaporative emissions.

The year 2000 saw over 500 million passenger cars in use worldwide with an annual worldwide production of new cars approaching 60 million. In addition, at the time of writing there are about 40% more passenger vehicles represented by trucks. The majority of these vehicles (automobiles and trucks) use a spark-ignited gasoline engine to provide power, and this has become the most frequent form of transportation. Gasoline blend still remains a mixture of paraffins and aromatic hydrocarbons that combust in air at a very high efficiency.

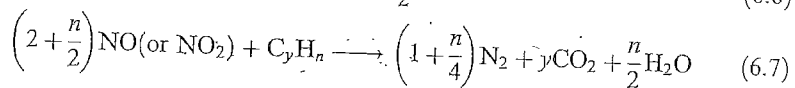
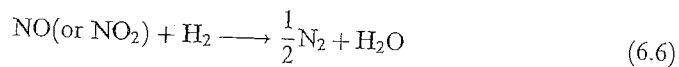
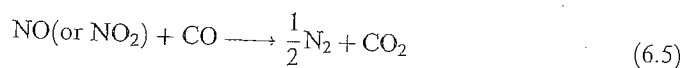
## 6.2 THE CATALYTIC REACTIONS FOR POLLUTION ABATEMENT

The basic operation of the catalyst is to perform the following reactions in the exhaust of the automobile:

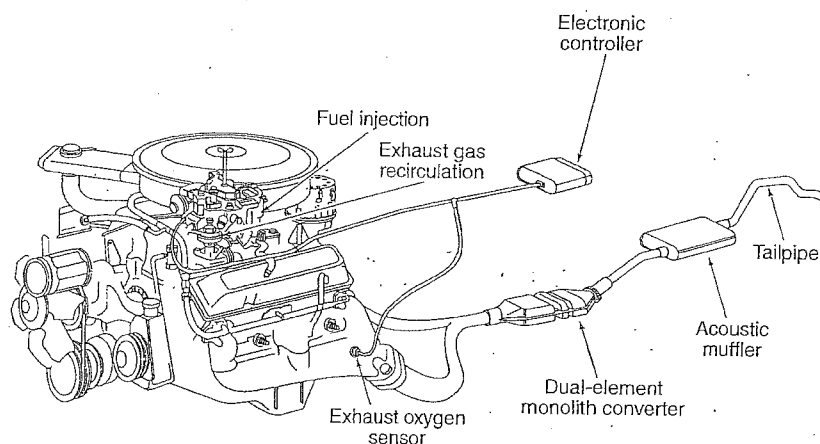
Oxidation of CO and HC to CO<sub>2</sub> and H<sub>2</sub>O:



Reduction of NO/NO<sub>2</sub> to N<sub>2</sub>:



The underbody location of the catalytic converter in the automobile is shown pictorially in Figure 6.2 (Mooney 1994). When a driver first starts the automobile, both the engine and catalyst are cold. As the exhaust gradually warms, it reaches a temperature high enough to initiate the catalytic reactions. This is referred to as the *lightoff temperature*, and the rate of reaction is kinetically controlled; that is, it depends on the chemistry of the catalyst since the transport reactions are fast. Typically, the CO (and H<sub>2</sub>) reaction begins first,



Closed-loop dual-catalyst system for emissions control using dual element monolith converter, which is three-way and oxidizing.

**Figure 6.2** Location of a catalyst in the underbody of an automobile. [Reprinted by permission of John Wiley & Sons, copyright © 1994 (Mooney 1994).]

followed by the HC and NO<sub>x</sub> reactions. When the vehicle exhaust is hot, the chemical reaction rates are fast, and pore diffusion and/or bulk mass transfer controls the overall conversion of the exhaust pollutants.

### 6.3 THE PHYSICAL STRUCTURE OF THE CATALYTIC CONVERTER

Both beaded (or particulate) and monolithic catalyst have been used for passenger vehicles from the onset of automotive emissions controls. In the United States, GM (General Motors) was the major company using spherical beads, while Ford and others used monoliths.

In parallel with all the studies related to catalyst screening, deactivation, and durability, there were many engineering issues that needed to be addressed in the early 1970s. How much backpressure would the presence of a catalytic reactor in the exhaust manifold contribute (increased backpressure translates to a loss in power and fuel economy)? Would the catalyst be able to maintain its physical integrity and shape in the extreme temperature and corrosive environment of the exhaust? How much weight would be added to the automobile, and what would be the effect on fuel economy? Another complicating problem was that the exhaust catalyst operation is in a continuously transient mode, in contrast to normal catalyst operation. These problems were critical because the consumer needed a cost-effective, highly reliable, trouble-free vehicle with readily delivered performance.

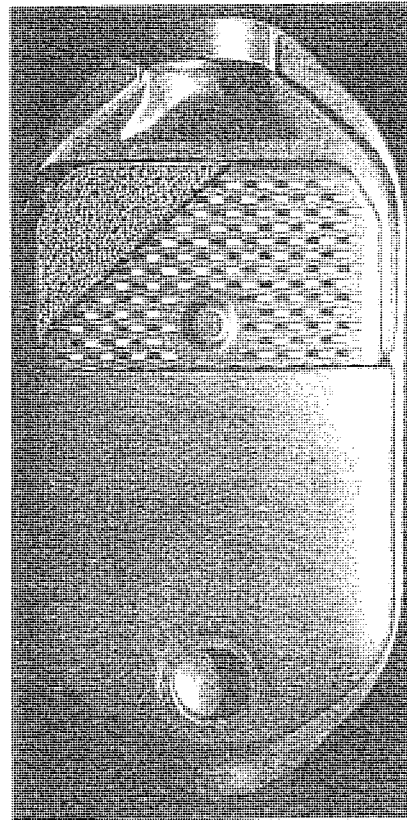


Figure 6.3 Bead bed reactor design. (Courtesy WR Grace & Co.)

### 6.3.1 The Beaded Catalyst

A quite important question that the engine manufacturers had to address is how to house the catalyst in the exhaust. The most traditional way was to use spherical particulate  $\gamma\text{-Al}_2\text{O}_3$  particles, anywhere from  $\frac{1}{8}$  to  $\frac{1}{4}$  in. in diameter, into which the stabilizers and active catalytic components (i.e., precious metals) would be incorporated. These "beads" would be mounted in a spring-loaded reactor bed downstream, just before the muffler. Since the engine exhaust gas was deficient in oxygen, air was added into the exhaust using an air pump. The rationale was simple—catalysts had been made on these types of supports for many years, and manufacturing facilities to mass produce them were already in place. There were known reactor designs and flow models that would make scaleup easy and reliable. One major concern was the attrition resistance of the  $\gamma\text{-Al}_2\text{O}_3$  particles, since they would experience many mechanical stresses during the lifetime of the converter. A typical bead bed reactor design for the early oxidation catalysts is shown in Figure 6.3.

The beads are manufactured with the stabilizers (discussed later) incorporated into the structure. The precious metal salts are impregnated into the bead and, using proprietary methods, fixed in particular locations to insure adequate performance and durability for 50,000 mi. They are then dried at typically 120°C, and calcined to about 500°C to their finished state. The finished catalyst usually had about 0.05 wt% precious metal with a Pt:Pd weight ratio of 2.5:1. After 1979 the need for NO<sub>x</sub> reduction required the introduction of small amounts of Rh into the second-generation catalysts. To control the levels of deactivation and performance of the bead catalysts, many studies were conducted on varying the location of the active catalysts within the bead structure (Hegedus and Gumbleton 1980).

### 6.3.2 The Honeycomb Catalyst

An alternative approach for supporting the catalytic components was that of a ceramic honeycomb monolith with parallel, open channels (see Figure 2.2, Chapter 2). In the mid-1960s, Engelhard began investigating the use of monolithic structures for reducing emissions from forklift trucks, mining vehicles, stationary engines, and so on (Cohn 1975). Catalyst preparation studies on these PTX purifiers formed the basis for washcoating technology for the automotive applications. The effects of operating temperature and feed impurities on catalyst durability were also determined. Some PTX converters had operational life of 10,000 h. This background experience showed that the monolithic support was a viable material for automotive applications. The precious metal  $\gamma$ -Al<sub>2</sub>O<sub>3</sub> catalyst was washcoated or deposited onto the walls of the honeycomb channels. A washcoated honeycomb typical of that used in the early catalytic converters is shown in Figure 2.2 in Chapter 2. One major advantage would be low-pressure drop, since the honeycomb structure had a very high open frontal area (~70%) and parallel channels. Furthermore, given their monolithic structure, they could be oriented in a number of ways to fit in the exhaust manifold. Also, the monoliths were available in different cell densities or cells per square inch (cpsi). From the experience in forklift trucks, there was a small database from which to design catalytic reactors. They offered potential flexibility, but naturally, the materials and geometries had to be optimized and designed for this new and very demanding application.

The ceramic companies continued to modify the materials and structures to provide sufficient strength and resistance to cracking under thermal shock conditions experienced during rapid acceleration and deceleration. The thermal shock condition was eventually satisfied by mechanical design coupled with the use of a low-thermal-expansion ceramic material called *cordierite* (synthetic cordierite has a composition approximating 2MgO, 5SiO<sub>2</sub>, and 2Al<sub>2</sub>O<sub>3</sub>). In preparing the catalyst, this desirable property has to be matched by the thermal expansion properties of the washcoat to prevent a mismatch in thermal properties. Monolithic structures were ultimately produced by a novel extrusion technique, which allowed mass production to be cost-effective. The first honey-

comb catalysts of large quantity to be used in automobile exhaust had 300 cells per square inch (cpsi), with wall thickness of about 0.012 in., and open frontal area of about 63%. These dimensions were finalized, on the basis of mechanical specifications and activity performance requirements, to ensure a high degree of contact between the reactants and the catalyst washcoat (high mass transfer) and the lowest possible lightoff temperature. Later developments in extrusion technology resulted in a 400-cpsi honeycomb with a wall thickness of 0.006 in. and open frontal area of 71%. This increased the geometric surface area for the mass-transfer-controlled reactions.

Catalyst companies began to explore these new structures as catalyst supports. They developed slurries of the catalytic coating that could be deposited onto the walls of the honeycomb, producing adherent "washcoats." The washcoat thickness could be kept at a minimum to decrease pore diffusion effects while allowing sufficient thickness for anticipated aging due to deposition of contaminants. The washcoat is about 20 and 60  $\mu\text{m}$  on the walls and corners (fillets), respectively. One method of preparing a washcoated honeycomb is to submerge it in a slightly acidified slurry (slip) containing the  $\gamma\text{-Al}_2\text{O}_3$  already impregnated with stabilizers and precious metals. The washcoat bonds chemically and physically to the honeycomb surface, where some of the washcoat fills the large pores of the ceramic. The slurry must have the proper particle size distribution to be compatible with the pores of the ceramic wall. Another method involves first washcoating the honeycomb with the alumina slurry, drying and calcining it, and then dipping it into the impregnating solutions. The coated honeycomb is air-dried, and calcined to about 450–500°C to ensure good adhesion. Typically, the catalyst contains about 0.1–0.15% precious metals. For the oxidation catalysts of the first generation, the weight ratio of Pt to Pd was 2.5:1, whereas the second generation contained a weight ratio of 5:1 Pt:Rh.

The honeycomb catalyst is mounted in a steel container with a resilient matting material wrapped around it to ensure vibration resistance and retention (Keith et al. 1969). Positive experience with honeycomb technologies has resulted in increased use of these structures over that of the beads, due to size and weight benefits. Today almost all automobiles are equipped with honeycomb-supported catalysts similar to that shown in Figure 6.4.

Although the early honeycombs were ceramic, recently metal substrates have been finding use because they can be made with thinner walls and have open frontal areas of close to 90%, allowing lower pressure drop. Cell densities greater than 400 cpsi can be used, which permits smaller catalyst volumes when higher cell densities are used. With some metal substrate suppliers, the catalyst is first coated onto the sheet metal and then fabricated into the honeycomb structure. This has the advantage of producing uniform coating thickness, thus eliminating the fillets. Because of expense and temperature limitations, these catalysts are not preferred. However, they are finding some markets because of their low-pressure-drop characteristics.

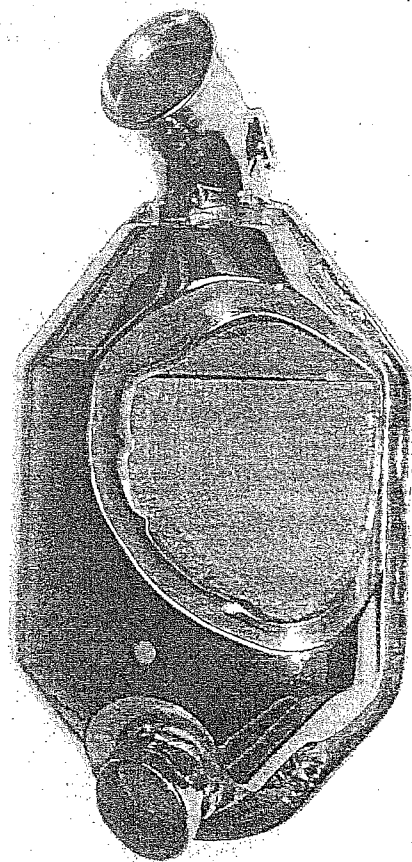


Figure 6.4 Monolithic reactor design. (Courtesy Engelhard Corp.)

By the year 2000, over 30 years of catalyst technology development had been devoted to the automotive exhaust catalyst. Figure 6.5 shows a typical automotive catalyst design.

These technology advances have been driven by the quest for a zero emission vehicle using the spark-ignited engine as the powertrain. Along with the advances in catalyst technology, the automotive engineers were developing new engine platforms and new sensor and control technology. This has resulted in the full integration of the catalyst into the emission control system. The catalyst has become integral in the design strategy for vehicle operation. During this time period the automotive catalyst has progressed through the following development phases.



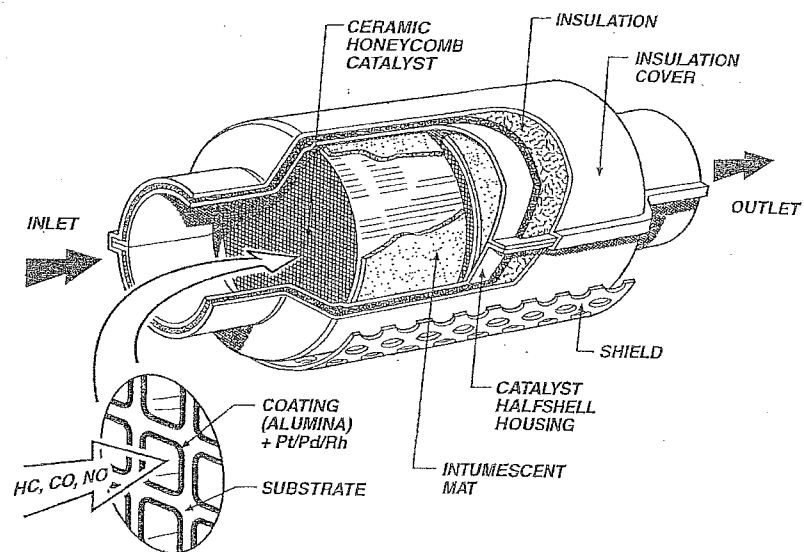
**THREE WAY CATALYST (TWC) DESIGN**

Figure 6.5 Schematic of cutaway of typical auto catalyst design. (Courtesy Engelhard Corp.)

- Oxidation catalyst
  - Bead and monolith support
  - HC and CO emissions only
  - Pt-based catalyst
  - Stabilized alumina
- ↓
- Three-way catalyst
  - HC, CO, and NO<sub>x</sub> emissions
  - Pt/Rh-based catalyst
  - Ce oxygen storage
- ↓
- High-temperature three-way catalyst
  - Approaching 950°C
  - Stabilized Ce with Zr
  - Pt/Rh, Pd/Rh, and Pt/Rh/Pd
- ↓
- All-palladium three-way catalyst
  - Layered coating
  - Stabilized Ce with Zr

↓

- Low-emission vehicles

High temperature, with/without Ce, close-coupled

Catalyst, approaching 1050°C

With underfloor catalyst

↓

- Ultra-low-emission vehicles

High temperature, with/without Ce, close-coupled catalyst, approaching 1050°C

Increased volume underfloor, higher precious-metal loading

Optional trap

#### 6.4 FIRST-GENERATION CONVERTERS: OXIDATION CATALYST (1976-1979)

During the early implementation of the Clean Air Act, the catalyst was only required to abate CO and HC. The  $\text{NO}_x$  standard was relaxed so engine manufacturers used exhaust gas recycle (EGR) to meet the  $\text{NO}_x$  standards. EGR dilutes the combustion gas and lowers the combustion flame temperature, which results in less thermal  $\text{NO}_x$  formation as predicted by the Zeldovich mechanism (Zeldovich 1946). The engine was operated just rich of stoichiometric to further reduce the formation of  $\text{NO}_x$ , and secondary air was pumped into the exhaust gas to provide sufficient  $\text{O}_2$  for the catalytic oxidation of CO and HC on the catalyst.

During this period, many catalytic materials were studied and the area of high-temperature stabilization of alumina was explored. It was known that the precious metals, Pt and Pd, were excellent oxidation catalysts; however, the cost and supply of these materials was bothersome. Therefore, many base metal candidates were investigated, such as Cu, Cr, Ni, and Mn. They were less active than the precious metals but substantially cheaper and more readily available (Yao 1975; Kummer 1975).

Table 6.1 shows the relative activities of Pt and Pd versus non-precious-metal oxides (base metal oxides) for oxidizing simulated exhaust pollutants at 300°C (Kummer 1975). From the relative activities, it is clear the precious metals are considerably more active than the base metals. Also, the activity depends on the species to be catalyzed. Palladium is the most active for CO and ethylene oxidation, whereas Pt is equally active for ethane oxidation. Precious metals would, therefore, be preferred over base metals if not for the expense and limited availability. The base metal oxides could be viable, but their lower activity would require larger reactor volumes (lower space velocities). This would be a problem in the engine exhaust underfloor piping where space is at a premium. Studies also showed that the base metal oxides were very susceptible to sulfur poisoning (Farrauto and Wedding 1974; Fishel et al. 1974; Taylor

TABLE 6.1 Comparison between Relative Activities of Precious-Metal and Base Metal Catalysts for Different Reactants<sup>a</sup>

Reactant	1% CO	0.1% C <sub>2</sub> H <sub>6</sub>	0.1% C <sub>2</sub> H <sub>8</sub>
Pd	500	100	1
Pt	100	12	1
Co <sub>2</sub> O <sub>3</sub>	80	0.6	0.05
CuO/Cr <sub>2</sub> O <sub>3</sub>	40	0.8	0.02
Au	15	0.3	<0.2
MnO <sub>2</sub>	4.4	0.04	—
CuO	45	0.6	—
LaCoO <sub>3</sub>	35	0.03	—
Fe <sub>2</sub> O <sub>3</sub>	0.4	0.006	—
Cr <sub>2</sub> O <sub>3</sub>	0.03	0.004	0.008
NiO	0.013	0.0007	0.0008

<sup>a</sup>Reaction in oxidizing atmosphere at 300°C.

Source: Kummer (1975); reprinted with permission, copyright © 1975, American Chemical Society.

1990). Interest still exists for Cu-based systems, as shown by ongoing studies (Kapteijn et al. 1993; Theis and LaBarge 1992).

Therefore, the first-generation oxidation catalysts were a combination of Pt and Pd and operated in the temperature range of 250–600°C, with space velocities varying during vehicle operation from 10,000 to 100,000 l/h, depending on the engine size and mode of the driving cycle (i.e., idle, cruise, or acceleration). Typical catalyst compositions were Pt and Pd in a 2.5:1 or 5:1 ratio ranging from 0.05 to 0.1 troy oz/car (a troy oz is ~31 g).

#### 6.4.1 Deactivation

The oxidation catalyst was negatively affected by the exhaust impurities of sulfur oxides and tetraethyl lead from the octane booster, both present in the gasoline, and phosphorus and zinc from engine lubricating oil (Doelph et al. 1975; Acres et al. 1975). An example of one of these studies (see Figures 6.6 and 6.7) shows the effect Pb, S, and thermal aging have on Pd versus Pt catalysts for the temperature at which 90% of the pollutant is converted (Doelph et al. 1975). The catalyst was formulated to have a constant 0.05 wt% total precious metal.

Clearly, the addition of Pt improved the resistance to Pb poisoning by showing a continuous decrease in the 90% conversion temperature. This study also noted an improvement in sulfur resistance for increases in Pd content. When the catalysts were aged in an oxidizing atmosphere at 982°C, the Pd catalyst retained more activity relative to Pt. Pt catalysts do sinter in oxidizing environments to a much greater degree than do Pd catalysts (Klimisch et al. 1975), so Pt loses activity relative to Pd after thermal aging at 982°C, as shown.

As the research was ongoing for improved catalyst compositions, the Pb present as an octane booster continued to deactivate most severely all the cat-

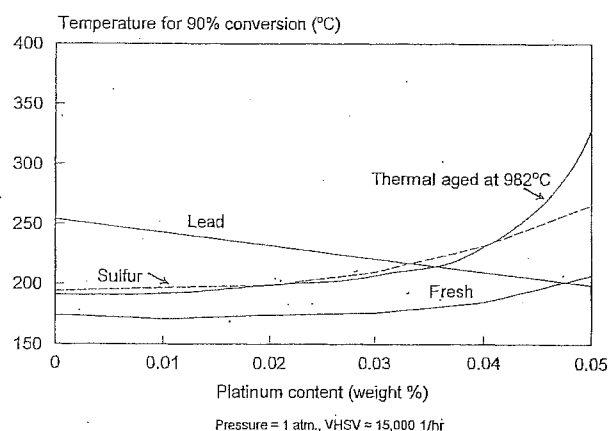


Figure 6.6 Effect of lead, sulfur, and thermal aging on carbon monoxide activity for Pt + Pd combined oxidation catalyst. [Reprinted with permission, © 1975 American Chemical Society (Doelph et al. 1975).]

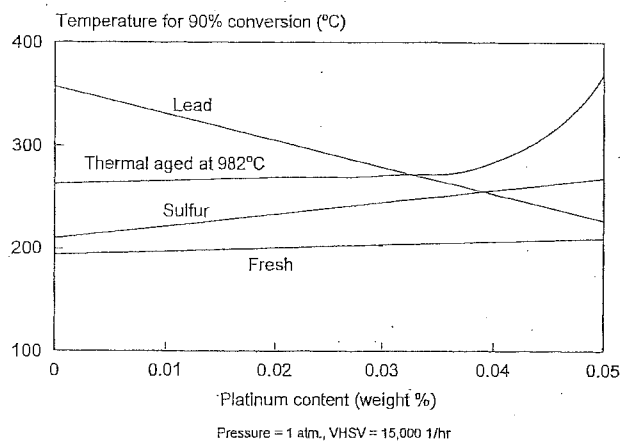
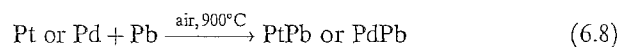


Figure 6.7 Effect of lead, sulfur, and thermal aging on propylene activity for Pt + Pd combined oxidation catalyst. [Reprinted with permission, © 1975 American Chemical Society (Doelph et al. 1975).]

alytic materials. Poisoning of Pt and Pd by traces of Pb (~3-4 mg/gal of Pb were in gasoline) was caused by formation of a low-activity alloy.



Electron microscopy studies showed that the Pb deposited primarily in a thin shell (a few micrometers thick) near the outer edge of the  $\text{Al}_2\text{O}_3$  carrier

and close to the gaseous interface. Studies revealed that the Pt was more tolerant than Pd to Pb poisoning, so preparation processes were developed that permitted the deposition of the Pt slightly below the surface, while the Pd had a deeper, subsurface penetration. Additional pore diffusion resistance was then introduced, and although causing a small activity penalty, it provided improved life of the catalyst.

While the studies on the automotive catalyst were proceeding, other environmental studies were conducted that showed the severe effect of lead present in the environment. There was a growing concern about Pb as a direct poison to humans. These studies contributed to the decision that led the federal government to mandate its removal from gasoline. This proved to be a benefit for automobile emission control. The use of catalysts was now more feasible in meeting the 50,000-mi performance requirements. It is interesting to note that the debate on removing lead from gasoline still continues as we begin to implement automobile emission control technologies in emerging countries such as India and China (MECA 1998).

However, the operating environment of the catalyst was still hostile in that phosphorus (P) and sulfur (S) were present, as well as the severe temperature transients and possible temperature exposure of 800–1000°C maximum.

The combinations of Pt and Pd dispersed onto high-surface-area  $\gamma$ -Al<sub>2</sub>O<sub>3</sub> particles were found to have reasonably good fresh activity. After high-temperature aging (900°C in air/steam to simulate engine exhaust conditions), the catalyst usually lost some of its activity, as evidenced by increased temperatures for 50% conversion of both CO and HC. Characterization of the partially deactivated catalyst by BET surface area measurements and X-ray diffraction patterns showed that the  $\gamma$ -Al<sub>2</sub>O<sub>3</sub> had undergone severe sintering to a lower surface area, more crystalline phase such as  $\alpha$ -Al<sub>2</sub>O<sub>3</sub> (see Chapter 2). The high area pore structure of the  $\gamma$ -Al<sub>2</sub>O<sub>3</sub> effectively collapses and occludes the active catalytic species, rendering them inaccessible to the reactants (see Chapter 5, Figure 5.3). Naturally, this results in a loss of catalytic performance. Since no other carrier materials had all the desirable properties of  $\gamma$ -Al<sub>2</sub>O<sub>3</sub>, research was directed toward understanding and minimizing the sintering mechanisms of  $\gamma$ -Al<sub>2</sub>O<sub>3</sub> under automobile exhaust conditions. It was known that certain contaminants such as Na and K acted as fluxes, accelerating the sintering process of  $\gamma$ -Al<sub>2</sub>O<sub>3</sub>. Thus, preparations had to exclude these elements. In contrast, small amounts (1–3%) of other elements such as La<sub>2</sub>O<sub>3</sub> (Kato et al. 1987; Tjburg et al. 1991), BaO (Machida et al. 1988), and SiO<sub>2</sub> (Beguín et al. 1991), if properly incorporated into the preparation process, had a stabilizing effect on the  $\gamma$ -Al<sub>2</sub>O<sub>3</sub> and significantly reduced its sintering rate. Figure 6.8 illustrates a representative response of the temperature to the BET surface area and compares some typical surface areas after high-temperature treatment at 1200°C, with and without stabilizers present (Wan and Dettling 1986a). Surface areas of 150–175 m<sup>2</sup>/g are typical for the aluminas in modern automotive catalysts.

Although the precise mechanism for their stabilizing effect is not known,

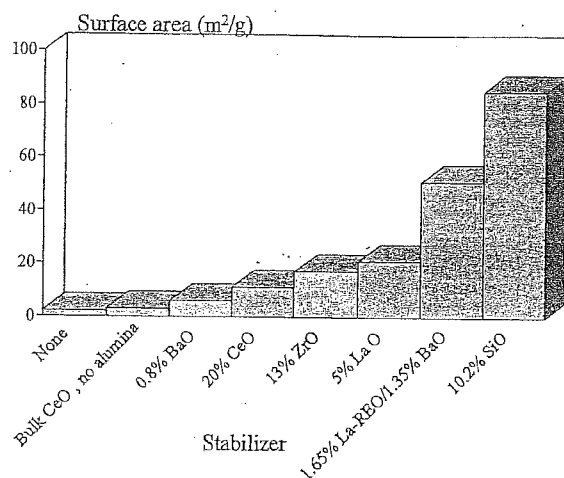


Figure 6.8 Thermal stabilization of aluminas for TWC automotive catalyst after 1200°C aging (Wan and Dettling 1986a, b).

high-resolution surface studies (Tijburg et al. 1991) have indicated that these oxides enter into the surface structure of the  $\gamma$ -Al<sub>2</sub>O<sub>3</sub> and greatly diminish the rate of the chemical and physical changes occurring normally during sintering.

The development of thermally stable high-surface-area  $\gamma$ -Al<sub>2</sub>O<sub>3</sub> by the incorporation of oxides was a breakthrough in materials technology, and its use uncovered another problem: agglomeration or sintering of the Pt and Pd during high-temperature exposure in the automobile exhaust (Wanke and Flynn 1975). Hydrogen chemisorption and XRD studies revealed that the Pt and Pd, initially well dispersed on stabilized  $\gamma$ -Al<sub>2</sub>O<sub>3</sub>, had undergone significant crystallization after high-temperature treatment. The Pd was more stable than the Pt as indicated in Figure 6.9 for CO conversion (Klimisch et al. 1975).

The first-generation oxidation catalysts consisted of 2.5:1 weight ratio of Pt:Pd at about 0.05% total precious metal for beads, and about 0.12% for honeycombs. Stabilizers such as CeO<sub>2</sub>, and La<sub>2</sub>O<sub>3</sub> were also included in the formulation to minimize sintering of the  $\gamma$ -Al<sub>2</sub>O<sub>3</sub> carrier.

## 6.5 NO<sub>x</sub>, CO, AND HC REDUCTION: THE SECOND GENERATION (1979–1986)

Following the successful implementation of catalysts for controlling CO and HC, the reduction of NO<sub>x</sub> emissions in the automobile exhaust to less than 1.0 g/mi had to be addressed. NO<sub>x</sub> reduction is most effective in the absence of O<sub>2</sub>, while the abatement of CO and HC requires O<sub>2</sub>. The exhaust emanating from the engine can be made sufficiently reducing (rich) so that a catalyst to



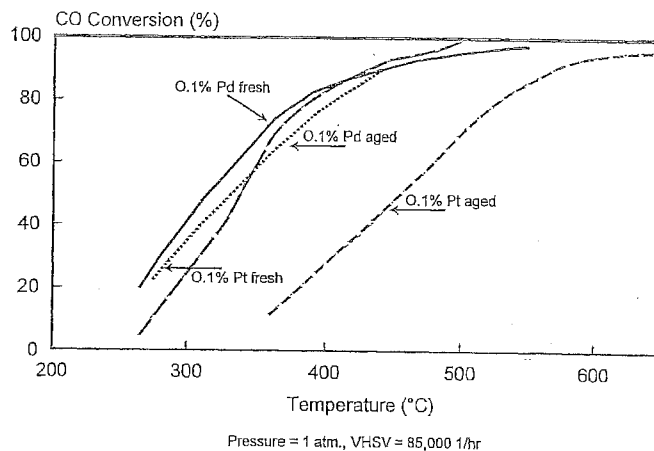


Figure 6.9 Effect of thermal aging of 70 h at 900°C for CO activity on Pt and Pd oxidation catalysts. [Reprinted with permission, © 1975, American Chemical Society (Klimisch et al. 1975).]

reduce  $\text{NO}_x$  could be positioned upstream of the air injection system in the exhaust and oxidizing catalyst. With this arrangement, the  $\text{H}_2$ , CO, and HC could first reduce the  $\text{NO}_x$ , and whatever amount remaining would be oxidized in the second bed. A primary catalyst for the reduction reaction was Ru; however, on an occasion when the engine exhaust might be oxidizing and the temperature exceeded about 700°C, it was found to volatilize by forming  $\text{RuO}_2$ . This was dropped from further consideration. When Pt or Pd was used instead of Ru, the  $\text{NO}_x$  was reduced to  $\text{NH}_3$  and not  $\text{N}_2$ . The  $\text{NH}_3$  would then enter the oxidation catalyst and be reconverted to  $\text{NO}_x$ . In previous studies of reducing atmospheres, Rh had also been shown to be an excellent  $\text{NO}_x$  reduction catalyst (Cohn 1964). It had less  $\text{NH}_3$  formation than Pt or Pd.

If the engine exhaust could be operated close to the stoichiometric air:fuel ratio, then all three pollutants (in theory) could be simultaneously converted, and the need for a two-stage reactor with air injection could be eliminated. Figure 6.10 shows such a curve in which the  $\text{NO}_x$  reduction occurs readily when the exhaust is rich, while the CO and HC reactions are prevented by insufficient  $\text{O}_2$ . As the air:fuel ratio approaches the stoichiometric point, there is a narrow window where simultaneous catalytic conversion of all three occurs. On the lean side, the CO and HC conversions are high, but at the sacrifice of the  $\text{NO}_x$ .

The key to advancing this technology was to control the air:fuel ratio of the automobile engine within this narrow window at all times. This was made possible by the development of the  $\text{O}_2$  sensor, which was positioned immediately before the catalyst in the exhaust manifold (Wang et al. 1993). The exhaust gas oxygen (EGO) or lambda sensor was composed of an anionic conductive solid

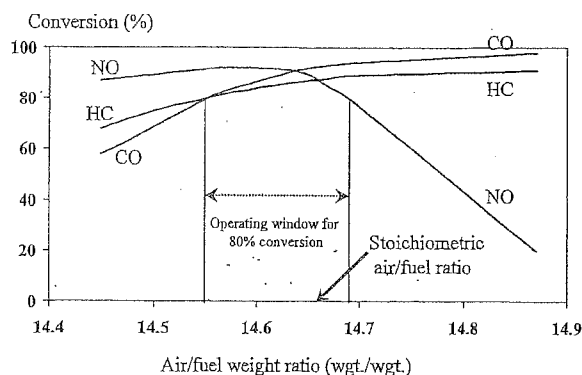


Figure 6.10 Simultaneous conversion of HC, CO, and NO<sub>x</sub> for TWC as a function of air:fuel ratio.

electrolyte of stabilized zirconia with electrodes of high-surface-area Pt. Very few solids are like stabilized ZrO<sub>2</sub>, which is an anionic 100% oxygen ion conductor. One electrode was located directly in the exhaust stream and sensed the O<sub>2</sub> content, while the second was a reference positioned outside the exhaust in the natural air. The electrode is a catalyst in that it converted the HC and CO at its surface, provided sufficient O<sub>2</sub> was present. For correct air/fuel control, the sensor must at all times equilibrate the exhaust gas. If the exhaust was rich, then the O<sub>2</sub> content at the electrode surface was quickly depleted. For the condition of a lean exhaust, O<sub>2</sub> remained unreacted, and the electrode sensed its relative high concentration. The voltage ( $E$ ) generated across the sensor was strongly dependent on the O<sub>2</sub> content and is represented by the Nernst equation. The sensor is an oxygen concentration cell:

$$E = E_0 + \frac{RT}{nF} \ln \frac{(PP_{O_2})_{\text{reference}}}{(PP_{O_2})_{\text{exhaust}}} \quad (6.9)$$

where  $n$  = number of electrons transferred

$F$  = Faraday constant

$E_0$  = standard state voltage

The voltage signal generated is fed back to the carburetor or to the fuel injection control device (i.e., throttle body injector or multipoint injectors), which adjusts the air:fuel ratio. Figure 6.11 shows the response profile for the O<sub>2</sub> sensor. Note that it functions similarly to a potentiometric titration curve used in aqueous analytic chemistry.

The total device is a very sophisticated electronic control system to maintain the air:fuel ratio within the narrow window, which allows the simultaneous conversion of all three pollutants. This technology, referred to as *three-way*

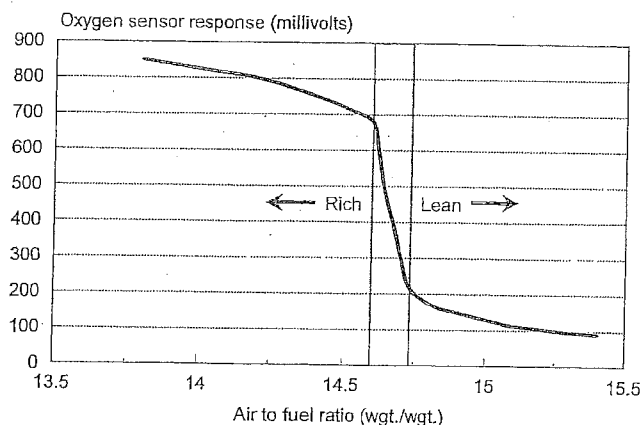


Figure 6.11 Oxygen sensor response output as a function of air: fuel ratio.

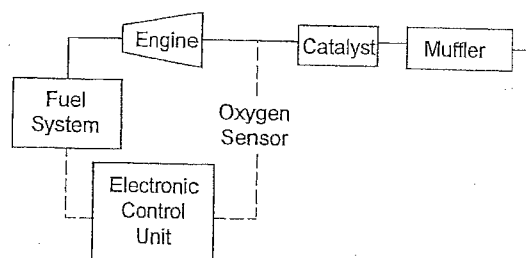


Figure 6.12 Major elements of the automotive feedback control system.

*catalysis* (TWC), was first installed in large quantities on vehicles in 1979. Even today, the oxygen sensor is the state of the art in air: fuel ratio control in the gasoline internal-combustion engine.

Modern sensors have been modified to be more poison tolerant to P and Si found in the engine exhaust. Also to improve the operating range of the  $O_2$  sensor during driving—particularly in cold start—the heated  $O_2$  sensor was developed (Wiedenmann et al. 1984). This is referred to as the *heated exhaust gas oxygen* (HEGO)-type sensor. A simple schematic of the vehicle control loop showing the exhaust catalyst and  $O_2$  sensor is illustrated in Figure 6.12.

Because the control system utilizes “feedback,” there is a time lag associated in adjusting the air: fuel (A/F) ratio. This results in a perturbation around the control setpoint. This perturbation is characterized by the amplitude of the A/F ratio and the response frequency (Hz).

A single catalyst technology to simultaneously convert all three pollutants was quickly developed. The primary precious metals were Pt and Rh; the latter were most responsible for reduction of  $NO_x$  (although it also contributes to CO

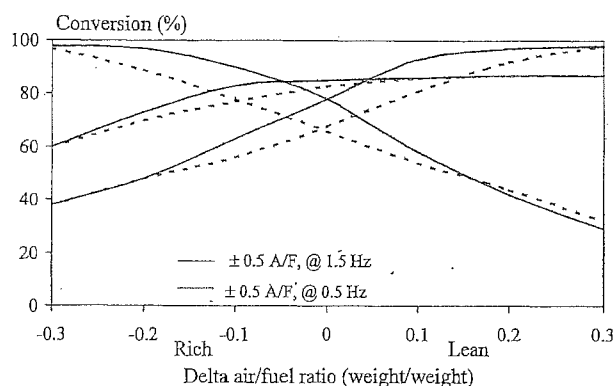
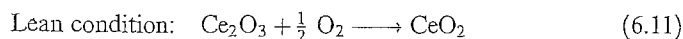


Figure 6.13 Increasing the perturbation frequency benefits TWC performance.

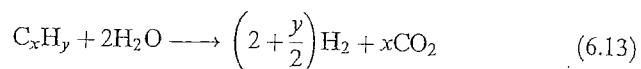
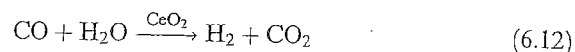
oxidation along with the Pt). The oscillatory nature of the A/F ratio in the exhaust means the catalyst alternatively will see slightly rich and slightly lean conditions.

The effect of this oscillation on an aged Pt/Rh containing TWC catalyst can be measured with an engine dynamometer test stand. The flow rate and temperature were kept constant, and the perturbation amplitude and frequency are varied. At steady state, the curves for CO, NO<sub>x</sub>, and HC conversion versus A/F ratio are very sharp, and the conversions are high. Increasing the amplitude causes a decrease in the absolute conversions and a broadening of the response curves. Similar results are seen by decreasing the frequency. The best control strategy to adapt to the engine is to have a small amplitude (<0.5 A/F) and a frequency greater than 1.5 Hz. Figure 6.13 shows the effect of frequency on the TWC catalyst performance. Note that all three reactants—CO, HC, and NO<sub>x</sub>—have higher conversions at lower amplitude (0.5 A/F) and higher frequency (1.5 Hz). Additional studies on the effects of the exhaust gas perturbation can be found in the literature (Heck et al. 1989; Kaneko et al. 1978; Falk and Mooney 1980; Schlatter et al. 1979; Muraki et al. 1985).

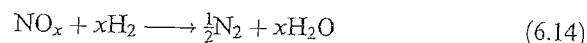
Thus, when operating rich, there was a need to provide a small amount of O<sub>2</sub> to consume the unreacted CO and HC. Conversely when the exhaust goes slightly oxidizing, the excess O<sub>2</sub> needs to be consumed. This was accomplished by the development of the O<sub>2</sub> storage component, which liberates or adsorbs O<sub>2</sub> during the air:fuel perturbations (Harrison et al. 1988; Fisher et al. 1993). CeO<sub>2</sub> was found to have the proper redox (reduction–oxidation) response and is the most commonly used O<sub>2</sub> storage component in modern three-way catalytic converters. The reactions are indicated below:



Another benefit of  $\text{CeO}_2$  is that it is a good steam-reforming catalyst and thus catalyzes the reactions of CO and HC with  $\text{H}_2\text{O}$  in the rich mode. The  $\text{H}_2$  formed then reduces a portion of the  $\text{NO}_x$  to  $\text{N}_2$ :



The hydrogen thus formed reduces  $\text{NO}_x$  via the following mechanism:



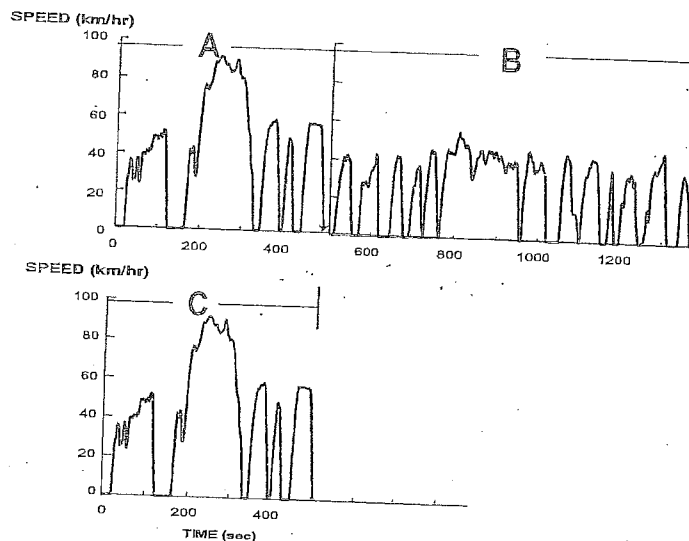
Other oxide materials with similar oxygen lability, such as  $\text{NiO}/\text{Ni}$  and  $\text{Fe}_2\text{O}_3/\text{FeO}$ , have also been used as storage components.

The modern three-way catalysts are composed primarily of  $\sim 0.1$ – $0.15\%$  precious metals at a Pt:Rh ratio of 5:1, high concentrations of bulk high surface area  $\text{CeO}_2$  (10–20%), and the remainder is the  $\gamma\text{-Al}_2\text{O}_3$  washcoat. The  $\gamma\text{-Al}_2\text{O}_3$  is stabilized with 1–2% of  $\text{La}_2\text{O}_3$ , and/or  $\text{BaO}$ . This composite washcoat is then deposited on a honeycomb with 400 cells per square inch. Typically, the washcoat loading is about 1.5–2.0 g/in.<sup>3</sup> or about 15% of the weight of the finished honeycomb catalyst. The size and shape of the final catalyst configuration varies with each automobile company but, typically, they are about 5–6 in. in diameter and 3–6 in. long.

## 6.6 VEHICLE TEST PROCEDURES (U.S., EUROPE, AND JAPAN)

The final performance tests for TWCs are the 1975 Federal Test Procedure (FTP) (Bosch 1993). This procedure was also used for the oxidation catalysts, but the interactions with the driving mode were not as predominate. This was because the vehicle often was lean-biased and/or oxygen was injected in the exhaust via an air pump, which decoupled the catalyst from the engine operation. However, for TWCs, any fluctuation in the engine operation changes the exhaust gas stoichiometry (A/F ratio) and dramatically affects catalyst performance.

The actual development of the 1975 FTP test procedure using a vehicle on a chassis dynamometer began in the 1950 time period. It evolved through the 1960s and finally, in 1975, was adapted by the EPA as the 1975 FTP. It is basically a driving cycle through Los Angeles, California and has the following characteristics:



Speed trace for 1975 Federal Test Procedure  
 Segment A: cold transient  
 Segment B: hot stabilized  
 Segment C: hot transient (after 10 minute soak)

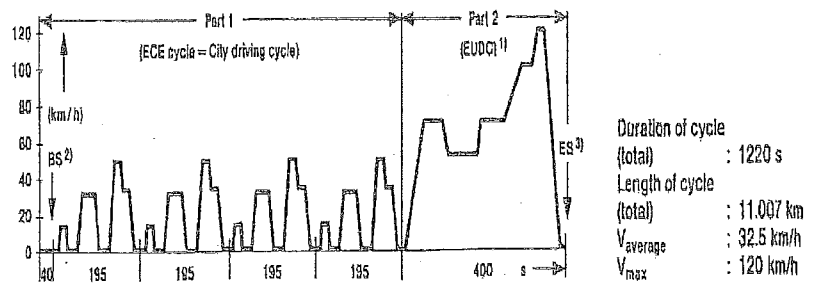
Figure 6.14 Speed trace for 1975 U.S. Federal Test Procedure. Segment A—cold transient; segment B—hot stabilized transient; segment C—hot transient (after 10-min soak).

Cycle length	11.115 mi
Cycle duration	1877 s plus 600-s pause
Bag 1	0–505 s
Bag 2	505–1370 s
Hot soak	600 s
Bag 3	0–505 s
Average speed	34.1 km/h
Maximum speed	91.2 km/h
Number of hills	23
Number of modes	112

Emissions are measured using a constant-volume sampling system. The test begins with a cold-start phase 1 or bag 1 (at 20–30°C) after a minimum 12-h soak at constant ambient temperature. After 505 s, the vehicle is driving at the speeds indicated in the phase 2 or bag 2 hot stabilized portion. The vehicle is then shut down for 600 seconds, after which the phase 3 cycle or bag 3 (hot start) is implemented. This phase is identical to the speeds and accelerations indicated in phase 1. The actual driving cycle is shown in Figure 6.14.

The driving cycles used for Japan and Europe are different from those of the 1975 FTP. These cycles are compared in the literature (Bosch 1993) and in





- 1) EUDC = Extra Urban Driving Cycle (EUDC)
- 2) Begin of sampling (after 40 s)
- 3) End of sampling (1220 s)

Note: 40 sec. idle eliminated for Stage III (2000) & Stage IV (2005) standards

Figure 6.15 European test driving cycles include ECE and EUDC: (1) extraurban driving cycle; (2) beginning of sampling (after 40 s); (3) end of sampling (after 1220 s).

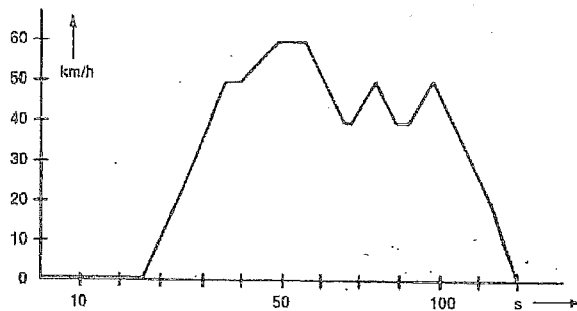
Figures 6.15 and 6.16. Note that the European test procedure shown in Figure 6.15 was revised to include the "cold start" or "key on" portion of the driving cycle. Prior European tests did not include emission sampling during the "cold start" portion.

The EPA recently conducted a test program to revise the 1975 FTP to reflect the high speed and acceleration driving habits of vehicle operators in the United States. The new Revised Federal Test Procedure (RFTP) contains two new test cycles to include driving encountered in the United States. The following excerpt from the *Federal Register* contains the rationale for these changes:

**SUMMARY:** This rulemaking revises the tailpipe emission portions of the Federal Test Procedure (FTP) for light-duty vehicles (LDVs) and light-duty trucks (LDTs). The primary new element of the rulemaking is a Supplemental Federal Test Procedure (SFTP) designed to address shortcomings with the current FTP in the representation of aggressive (high speed and/or high acceleration) driving behavior, rapid speed fluctuations, driving behavior following startup, and use of air conditioning. An element of the rulemaking that also affects the preexisting "conventional" FTP is a new set of requirements designed to more accurately reflect real road forces on the test dynamometer.

The U.S. SFTP portion that simulates high speed and rapid acceleration is the US06, while the portion that simulates the added engine load from air conditioner operation is the SC03. These new test cycles are shown in Figures 6.17 and 6.18.

## 1. 11-mode Cycle

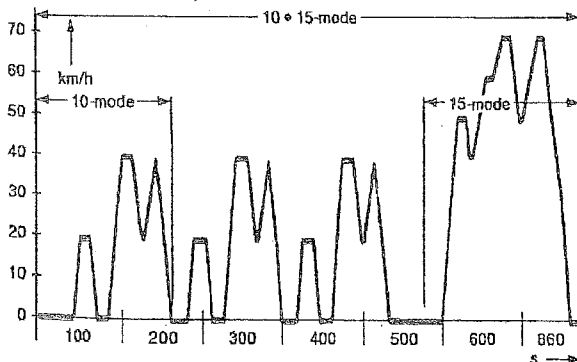


duration of cycle : 120 s  
 distance per cycle : 1.021 km  
 no. of cycles/test : 4  
 total test time : 505 s  
 total distance : 4.084 km  
 average speed : 30.6 km/h (39.1 km/h) \*)  
 max. speed : 60 km/h  
 \*) without idle phases (idle time = 21.7%)

**11-mode cold start test:** The 11-mode cycle is to be run 4 times, measurements are taken in all 4 cycles. After cold start 25 s. idle. The transmission gears to be used are specified for 3- and 4-speed transmissions. For special transmissions the gear ratios to be used are specified individually; for automatic transmissions only position "Drive". Exhaust emission analysis with CVS-system.

(a)

## 2. 10 • 15-mode Cycle



duration of cycle : 660 s  
 distance per cycle : 4.16 km  
 no. of cycles/test : 1  
 average speed : 22.7 km/h (33.1 km/h) \*)  
 max. speed : 70 km/h  
 \*) without idle phases (idle time = 31.7%)

**10 • 15-mode hot start test:** Preconditioning 15 min. with 60 km/h, followed by 5 min. at 60 km/h and one 15-mode cycle. After the preconditioning the combined 10 • 15-mode (3 cycles 10-mode plus 1 cycle 15-mode) is to be run and measured once.

(b)

Figure 6.16 The Japanese test driving cycle has two modes: (a) 11-mode cycle; (b) 10-15-mode cycle.

The transients in each engine chassis dynamometer driving cycle consist of changes in exhaust composition, temperature, speed, and air:fuel ratio. Figure 6.19 shows the indicated transients for speed, temperature, and air:fuel ratio for a 1996 Lincoln Towncar during the U.S. FTP. The actual vehicle control

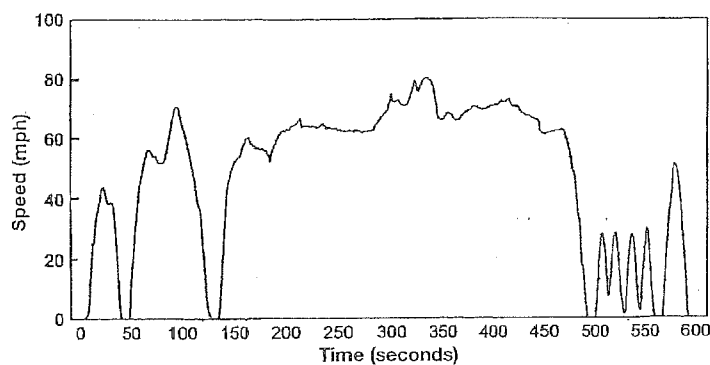


Figure 6.17 U.S. SFTP test cycle—US06 portion simulates high speed driving.

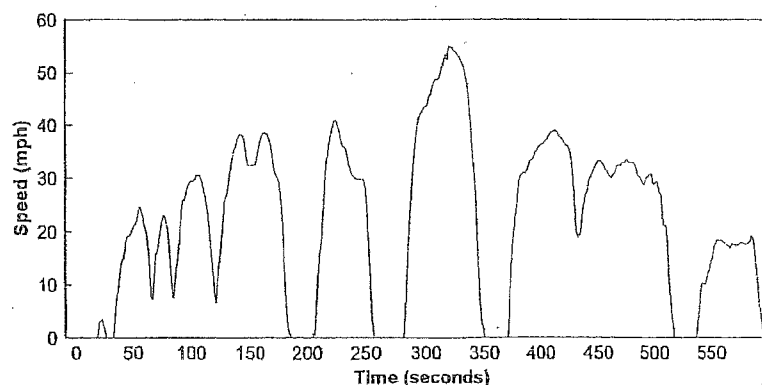


Figure 6.18 U.S. SFTP test cycle—SC03 portion simulates high speed driving.

strategy is different for each model and manufacturer. This results in different perturbations and different transient responses in the exhaust environment of the TWC catalyst. The effect of these variables has been studied for commercial vehicles with widely different control strategies (Adomaitis and Heck 1988).

### 6.7 NO<sub>x</sub>, CO, AND HC REDUCTION: THE THIRD GENERATION (1986–1992)

The latter part of 1980 and the early 1990s required improvement in technology because of the automobile's changing operational strategies; fuel economy was important, yet operating speeds were higher. This situation resulted in higher exposure temperatures to the TWC catalyst. Higher fuel economy was met by introducing a driving strategy whereby fuel is shut off during deceleration. The catalyst, therefore, is exposed to a highly oxidizing atmosphere that results in

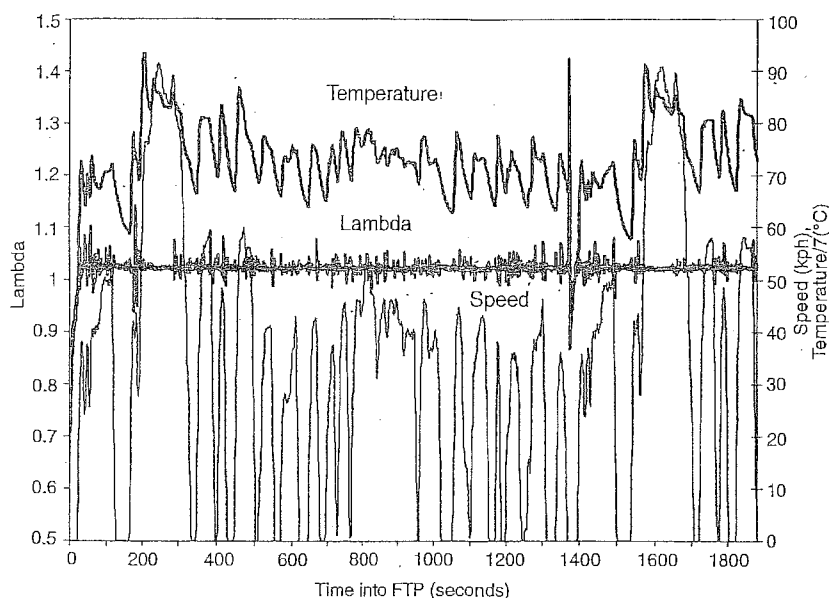


Figure 6.19 Transient response of air:fuel ratio, exhaust temperature, and speed of 1996 Lincoln Towncar during 1975 FTP.

deactivation of the Rh function by reaction with the  $\gamma$ -alumina, forming an inactive rhodium-aluminate species.

To simulate these modes of deactivation in the laboratory, engine dynamometer aging cycles were set up to simulate 50,000-mi performance. These aging cycles consisted of repetitive steps of changing the engine speed/load, air:fuel ratio, and exhaust temperature. In some cases, air was injected downstream into the exhaust, while in others the engine was connected to a flywheel and actual fuel cut was simulated. In addition, some cycles were isothermal, while others were exothermal, generating a large temperature rise on the catalyst surface. Figure 6.20 summarizes of the engine-out stoichiometry for the two different types of aging cycles.

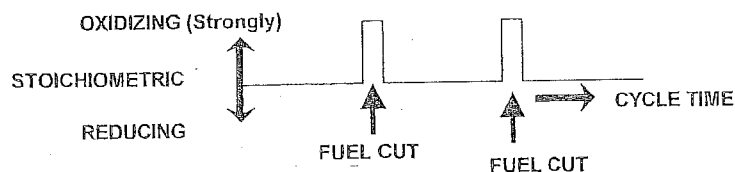
For aging cycles simulating fuel cut, the engine load is adjusted to give catalyst inlet temperatures ranging from 750 to 950°C. This cycle is essentially isothermal with respect to the catalyst surface temperature. The aging cycles generating an exotherm on the catalyst surface usually have an inlet temperature of 650–750°C, with catalyst bed temperatures ranging from 750 to 1000°C, depending on the concentration of the CO in the engine exhaust. The bed temperature is measured 1.0–1.5 in. from the start of the catalyzed honeycomb. Still other cycles studied accelerated poisoning of the catalyst by doping the lubricating oil with high concentrations of phosphorous.

Several studies have been conducted on the effect these various aging cycles have on the TWC performance (Carol et al. 1989; Heck et al. 1992; Skowron

## Engine Aging Cycles

(LEGEND: — ENGINE OUT, — CATALYST)

TYPE 1: TEMPERATURE = f(ENGINE EXHAUST)



TYPE 2: TEMPERATURE = f(REACTION EXOTHERM)

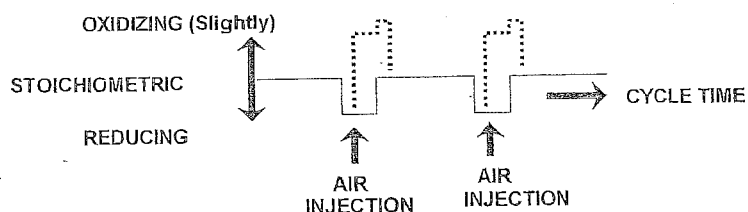


Figure 6.20 Description of engine dynamometer aging cycles.

et al. 1989; Hammerle and Wu 1984; Taylor 1993). One clear observation is the strong effect of aging temperature and exhaust gas oxygen concentration as shown in Figures 6.21 and 6.22 (Heck et al. 1992).

Studies have been conducted to reduce the reaction of Rh with high-surface-area carriers such as stabilized  $\gamma\text{-Al}_2\text{O}_3$ . At temperatures in excess of 800–900°C, in an oxidizing mode, the Rh reacts with the  $\text{Al}_2\text{O}_3$ , forming the inactive aluminate. Fortunately, this reaction is partially reversible, so in the rich mode some of the Rh is released from the aluminate:

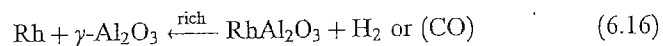
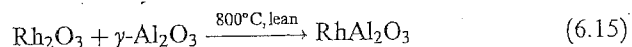


Figure 6.23 illustrates the effect of rich and lean treatments on the performance of a modern TWC catalyst. This catalyst was aged on a fuel-cut engine aging cycle at 850°C inlet temperature. It was subsequently exposed to rich engine exhaust at 850°C and evaluated using a sweep test. A sweep test is a very convenient test conducted on an engine dynamometer, and the conversion

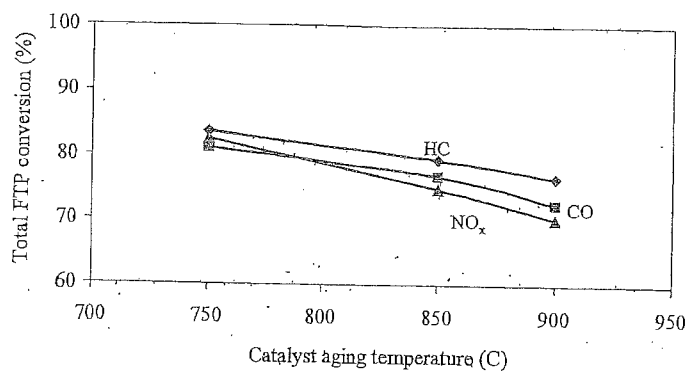


Figure 6.21 Aging temperature negatively affects total FTP performance with fuel-cut aging. [Reprinted with permission, © 1992 Society of Automotive Engineers, Inc. (Heck et al. 1992).]

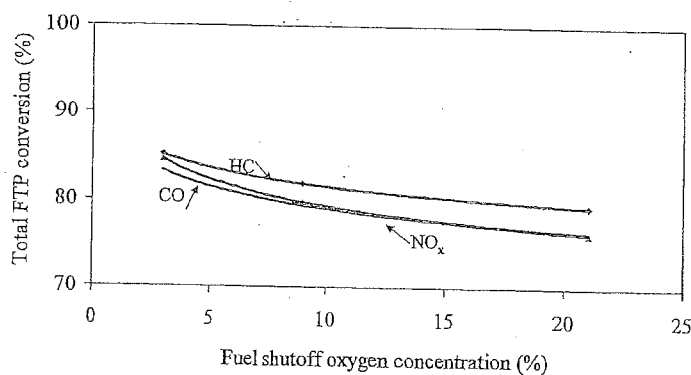


Figure 6.22 Fuel shutoff oxygen concentration affects total FTP performance with fuel-cut aging. [Reprinted with permission, © 1992 Society of Automotive Engineers, Inc. (Heck et al. 1992).]

across the catalyst is measured for various air:fuel ratios going from lean to rich engine operation. Exhaust temperature and flowrates are kept constant during the test sequence, while the perturbation amplitude and frequency can be varied. The test catalyst was then exposed to lean engine exhaust, and then again evaluated, and then again exposed to rich engine exhaust. The catalyst essentially recovers its activity. This reversible cycling suggests some form of facile complex is being formed with the Rh. The mechanism for Rh catalyst deactivation is still a subject of ongoing research (Wong and Tsang 1992; Wong and McCabe 1989).

A number of approaches to minimize these undesirable reactions are currently under investigation. A promising route appears to be to deposit the Rh

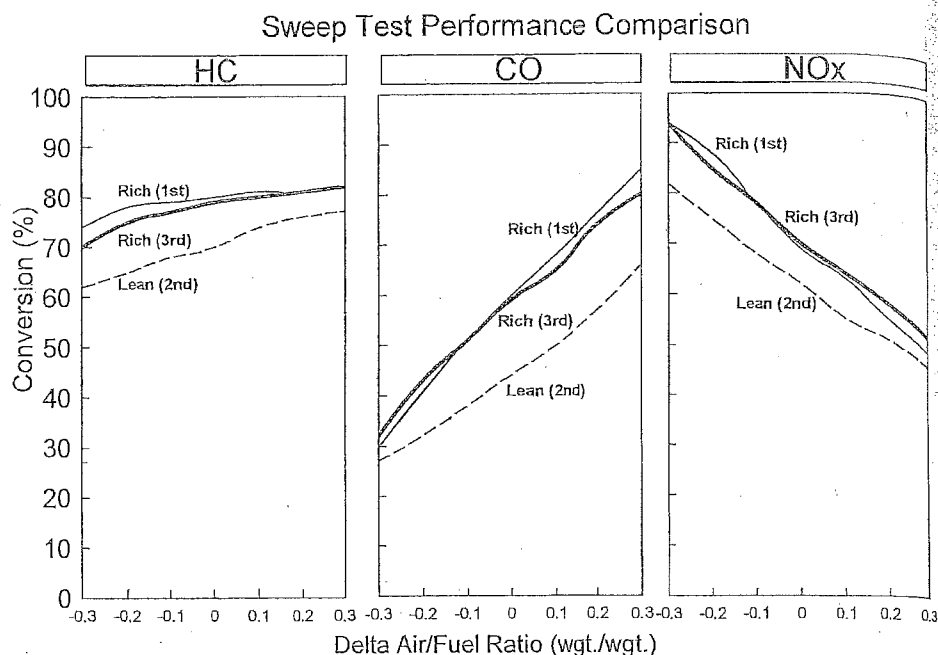


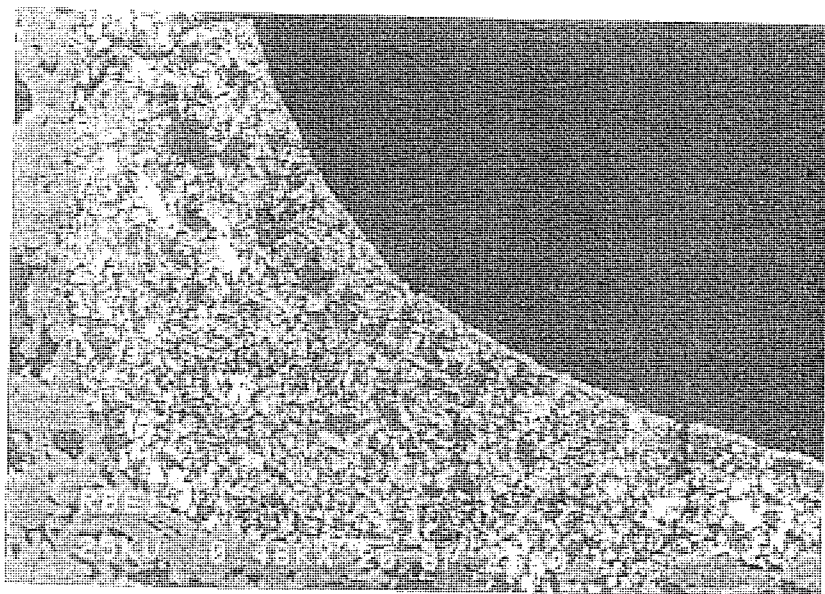
Figure 6.23 Fuel-rich engine operation regenerates rhodium activity after deactivation from lean exposure.

on a less reactive carrier such as  $\text{ZrO}_2$ . The catalyst companies consider the exact technology used to be highly confidential.

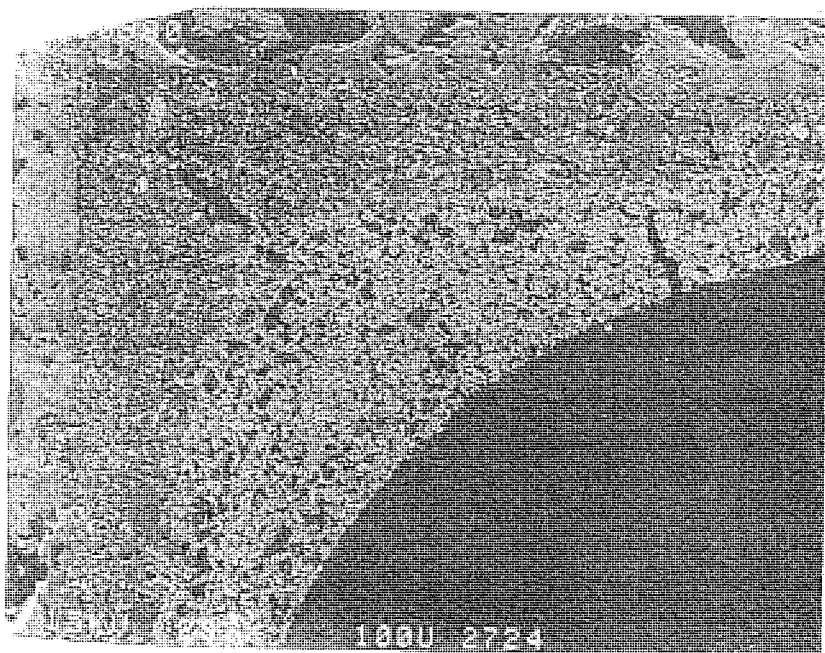
Another observation with regard to Rh stabilization is its possible interaction with  $\text{CeO}_2$ , the oxygen storage component (Wan and Dettling 1986b). During high-temperature lean excursions, the Rh can react with the rare earth oxide, reducing the activity of both species. Segregating the Rh is suggested as a way to improve tolerance to high-temperature lean excursions. This has resulted in multiple layers of washcoats with the Rh and  $\text{CeO}_2$  in different layers. Figure 6.24 shows micrographs of a single- and double-washcoat TWC catalyst for comparison. Studies have also been conducted on ways to stabilize the Ce with oxides of Zr, Ba, and La, and prevent interaction with the Rh catalyst (Funabiki et al. 1991; Usmen et al. 1992; Kubsh et al. 1991).

Additional studies centered on optimizing the ceria location (Ihara et al. 1990). These authors recommended placing the Ce adjacent to the opening of the aluminum pores. They also recommended separating the Ce from the precious metal in a layered catalyst.

Catalyst deactivation and reaction inhibition due to P and S, respectively, are still concerns in modern TWC catalysts (Gandhi and Shelef 1991; Brett et al. 1989). The phosphorous present in the lubricating oil as zinc dialkyldithiophosphate (ZDDP) deposits on the catalyst and results in deactivation. When it



(a)



(b)

Figure 6.24 SEM micrographs: preparation of TWC with single-coat (a) and double-coat (b) layers of catalyst.



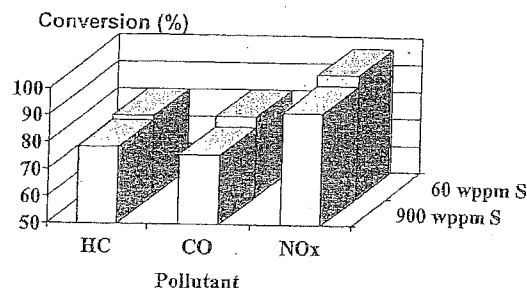


Figure 6.25 Sulfur in gasoline negatively affects FTP performance of TWC.

exits the combustion chamber, it usually deposits as a  $P_2O_5$  film or polymeric glaze on the outer surface of the  $Al_2O_3$  carrier, causing pore blockage and masking. This introduces pore diffusion limitations, and in the worst-case masking, which physically blocks reactant molecules from access to the active Pt, Rh, and Pd sites within the pore structure of the  $Al_2O_3$ . This continues to be a serious problem in many converters, but optimization of the pore structure of the  $Al_2O_3$  provides improved life to the catalyst. A small loss in activity results from the decrease in surface area as the smaller pores are occluded (Jobson et al. 1991; Williamson et al. 1985). Some studies have also considered the effect of silicon from various lubricants on catalyst performance (Ghandi et al. 1986).

Gasoline averages anywhere from 200 to 500 ppm (0.02–0.05%) and can contain up to 1200 ppm organosulfur compounds, which convert to  $SO_2$  and  $SO_3$  during combustion. The  $SO_2$  adsorbs onto the precious-metal sites at temperatures below about 300°C and inhibits the catalytic conversions of CO,  $NO_x$ , and HC. At higher temperatures, the  $SO_2$  is converted to  $SO_3$ , which either passes through the catalyst bed or can react with the  $Al_2O_3$  forming  $Al_2(SO_4)_3$ . The latter is a large-volume, low-density material that alters the  $Al_2O_3$  high area surface leading to catalyst deactivation. In addition, the  $SO_3$  can react with Ce and other rare earths. The effect of sulfur on the TWC catalyst has been studied (Beck et al. 1991). The actual effect of sulfur on a TWC catalyst performance in an FTP test is given in Figure 6.25 for nominally 60 wppm and 900 wppm sulfur in the gasoline. The impact of sulfur in the fuel has also been studied in fleet tests, and preliminary findings indicate that a significant reduction in both HC and CO emissions is obtainable by reducing the fuel sulfur level from 50 ppm down to 10 ppm (Colucci and Wise 1993). A study with the California phase 2 gasoline further points out the benefits of lowering the fuel sulfur content to 40 ppm (Lippincott et al. 1994; Calvert et al. 1993). This study looked at reformulated fuels and the major impact was identified as reduction in sulfur and fuel vapor pressure. These studies are ongoing as the push for lower sulfur fuels continues to be a strong issue regarding catalyst performance (Sawyer et al. 1992).

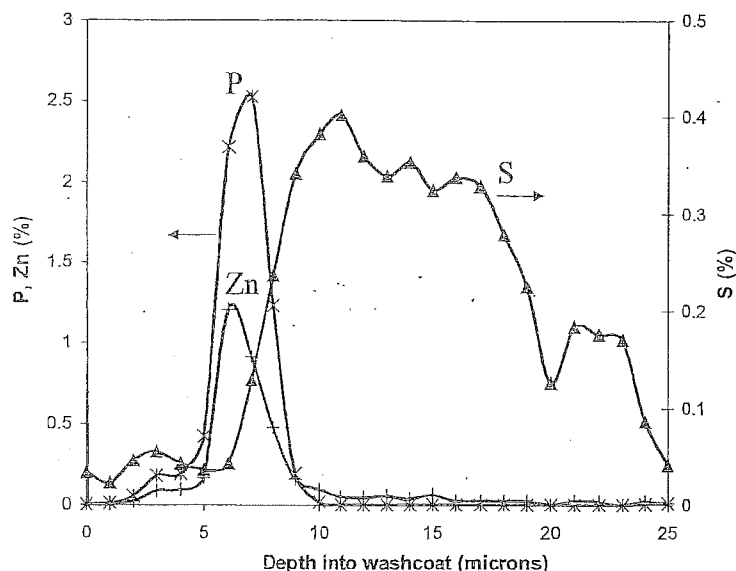


Figure 6.26 Concentration profiles of sulfur, phosphorus, and zinc in washcoat at inlet section of vehicle-aged TWC. [Reprinted with permission of the Royal Society of Chemistry (Heck and Farrauto 1994).]

Typical profiles of S, P, and Zn on deposits in the washcoat at an inlet and outlet section of a vehicle-aged catalyst are shown in Figures 6.26 and 6.27. The concentrations of S, P, and Zn are much greater in the inlet than the outlet section, indicating that the former serves as a filter. The sulfur is uniformly present throughout the washcoat, suggesting an interaction between it and the  $\text{Al}_2\text{O}_3$ . The P and Zn are concentrated near the outer periphery of the washcoat, but only in the inlet section. The drop in poison concentrations at  $\sim 20 \mu\text{m}$  is at the washcoat/monolith interface.

The TWC composition has an interesting effect on the sulfur compounds present in the exhaust. The  $\text{SO}_2$  is oxidized in the lean mode, forming  $\text{SO}_3$ , which reacts with  $\text{Al}_2\text{O}_3$  or  $\text{CeO}_2$ , forming  $\text{Al}_2(\text{SO}_4)_3$  or  $\text{Ce}(\text{SO}_4)_2$ . When the exhaust becomes rich, the sulfate compounds are reduced and form the unpleasant-smelling  $\text{H}_2\text{S}$ . Catalyst companies have developed technology to capture the  $\text{H}_2\text{S}$  before it is released to the atmosphere.

It appears that the main mechanism of release of  $\text{H}_2\text{S}$  is through the Ce. Studies have looked at modifications of the Ce through thermal treatment (Lox et al. 1989). This treatment changes the crystallite size and reduces the number of surface hydroxyl groups, thus lowering the retained sulfur oxides. Other studies have looked at scavengers that actually remove the  $\text{H}_2\text{S}$ . Materials such as Ni have been found to be effective (Golunski and Roth 1991; Dettling et al. 1990).

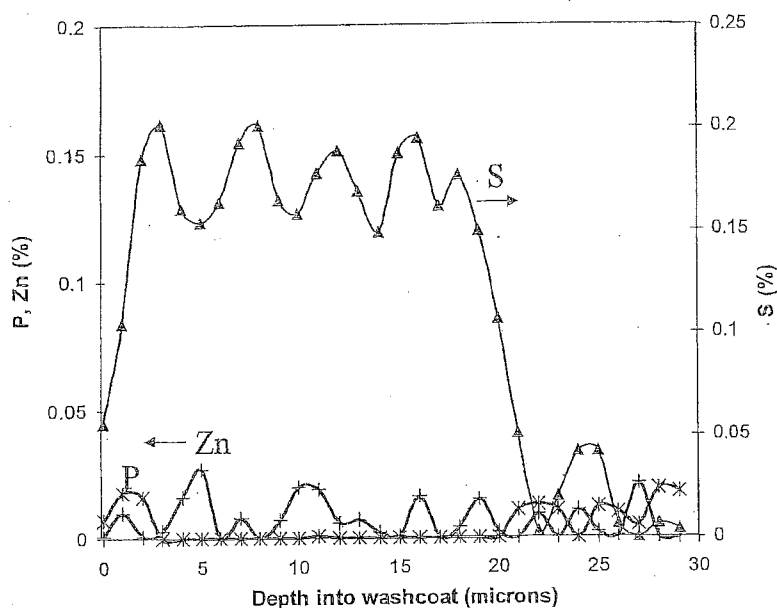


Figure 6.27 Concentration profiles of sulfur, phosphorus, and zinc in washcoat at outlet section of vehicle-aged TWC. Reprinted with permission of the Royal Society of Chemistry (Heck and Farrauto 1994).

#### 6.8 PALLADIUM TWC CATALYST: THE FOURTH GENERATION (MID-1990s)

Throughout the development of the automotive catalyst, the use of Pd as a replacement for Pt and/or Rh has been desirable because it is considerably less expensive than either. Its effectiveness for reducing hydrocarbon emissions for the more stringent standards has also been recognized (Yamada et al. 1993). One of the first changes in the conventional TWC technology was the substitution of Pd for Pt and the use of the Pd/Rh catalyst for certain commercial automotive applications (Lui and Dettling 1993; Dettling and Lui 1992). In the early 1990s, an effort was made to further reduce the cost of TWC's, so Pd was substituted for Rh, yielding a Pt/Pd catalyst (Lui and Dettling 1993). Performance of these catalysts was satisfactory under very restrictive operating conditions. However, when the cost of Rh reached >\$5000/troy oz in the late 1980s, more studies with Rh replacement in mind were conducted (Summers et al. 1988, Muraki 1991). This was not an easy task, and many researchers concluded that there was not a direct substitution for Rh among the precious-metal groups (Fisher et al. 1992). However, a number of changes were occurring in the strategies of the automobile for emission control to meet TLEV and LEV, some of which proved beneficial for substituting Pd for Rh. Basically, the ve-

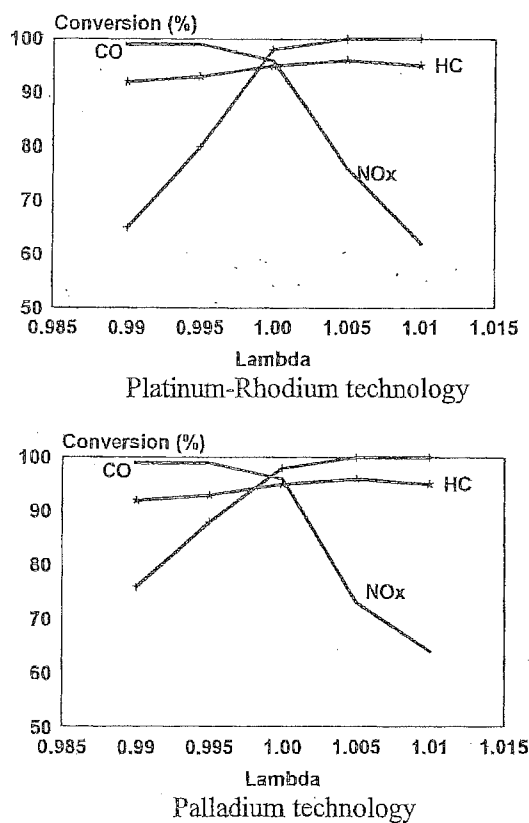


Figure 6.28 Performance of Pd-only TWC is comparable to that of Pt/Rh TWC on sweep test (Dettling et al. 1994).

hicles were being designed to have a very tight air:fuel perturbation, resulting in very small amplitudes and a high-frequency response. Fuel quality also was improving in by further reductions in the lead content. Concurrently, the catalysts were being placed closer to the manifold, giving faster heatup of the catalyst and higher steady-state operating temperatures. This diminished the adsorption of impurities such as sulfur and phosphorous (Heck et al. 1989).

There were some false starts during this period relative to announcements of the suitability of all Pd catalysts. However, the first real evidence of data giving performance and road durability was published in 1993 (Summers and Williamson 1993). This study showed that the Pd technology gave good performance after fuel-cut aging cycles and was not sensitive to sulfur in the exhaust gas. The advances in Pd technology continued at a rapid pace, and the first real commercial installations were in the 1995 model year for Ford (Hepburn et al. 1994). The key success to this new Pd technology is shown in Figure 6.28,

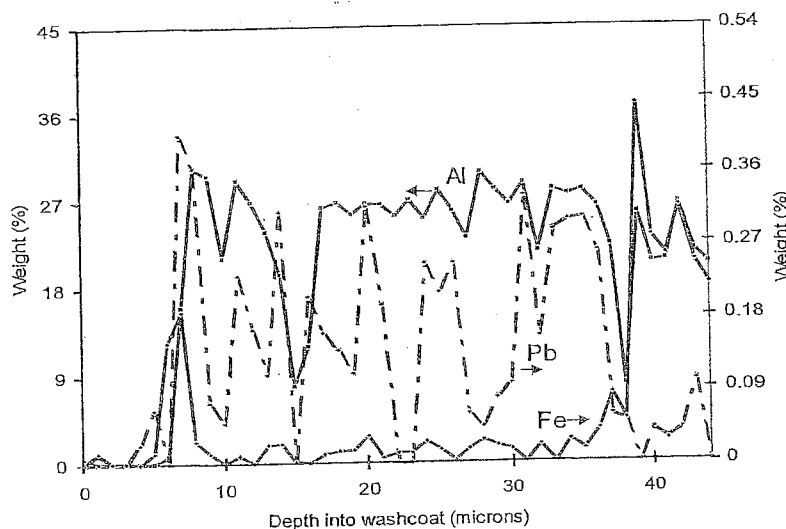


Figure 6.29 Pd catalyst performance is affected by residual Pb in gasoline pool (Sung et al. 1998).

which compares the performance of the all Pd technology with the commercial Pt/Rh technology (Dettling et al. 1994). The rich side activities for HC, CO, and NO<sub>x</sub> are equivalent for both catalyst technologies. All previous results on Pd catalysts showed lower performance on the rich side and therefore a much narrower operating window for high performance (Heck et al. 1989). The special combinations of stabilized ceria and washcoat components give this Pd catalyst equivalent performance at both loose and tight control perturbation conditions. The use of Pd catalyst continued to expand especially for vehicles having catalysts at the higher operating temperatures and possessing tighter air:fuel control strategies.

One caution continues with Pd-only TWC catalyst. In geographic locations where Pb continues to be in the gasoline source, Pd-only catalysts are susceptible to Pb poisoning. In one study of modern Pd TWC formulations, catalysts were aged with leaded fuel to determine effect on activity (Sung et al. 1998). Lead was found on the aged catalysts and was on the surface of the washcoat coatings and did penetrate within the washcoat, and was more predominant in the inlet section of the catalyzed monolith (see Figure 6.29). The impact of the Pb was mainly on NO<sub>x</sub> performance. TEM elemental mapping and XPS results suggest that Pb preferentially associates with the Pd. Adding Rh to the Pd catalyst improved the resistance to Pb and the catalyst performance especially for NO<sub>x</sub> conversion.

At the end of the twentieth century, the shift to a higher price of Pd combined with the short supply from the mine source resulted in a reevaluation of the use of Pd. Pt began to be substituted for Pd particularly in underfloor lo-

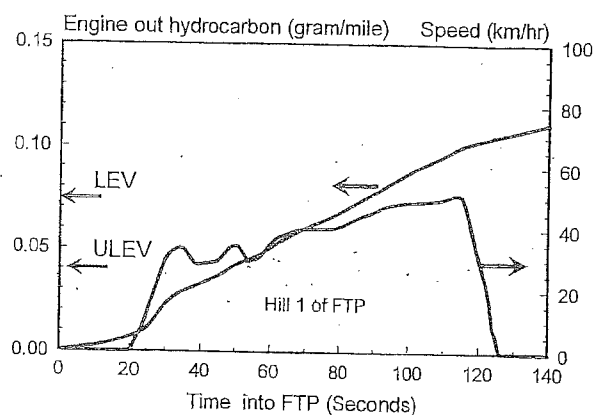


Figure 6.30 Cold-start emission control is the key to low-emission vehicles.

cations. So it has become very obvious that any future shift in technologies will be governed again by the price/supply issues among the various precious metals: Pd, Pt, and Rh.

## 6.9 LOW-EMISSION CATALYST TECHNOLOGIES

In order to accomplish the low emissions formulated by CARB for ULEV and SULEV vehicles, a number of approaches have been investigated in the mid to late 1990s. The emphasis of the new regulations was the reduction of HCs in the exhaust. A majority of hydrocarbon emissions (60–80% of the total emitted) are produced in the cold-start portion of the automobile, that is, in the first 2 min of operation. Typical composition of the hydrocarbons during cold start is as follows (Kumitake et al. 1996):

Hydrocarbon Type	Sampling Time (seconds after cold start), Approximate Hydrocarbon Composition (%)	
	3 s	30 s
Paraffins	20	35
Olefins	45	20
Aromatics, C6, C7	20	20
Aromatics, >C8	15	25

For a typical four-cylinder gasoline engine, the engine-out emissions in the FTP are shown in Figure 6.30. Also shown on this figure are the LEV and ULEV

emission regulations. Note that the emissions control device must be functional in 50 s (for ULEV) to 80 s (for LEV) to meet the low-emissions (LEV) standards.

The technology race to develop suitable methods to control cold-start hydrocarbons included both catalytic and some unique system approaches:

1. Close-coupled catalyst
2. Electrically heated catalyzed metal monolith
3. Hydrocarbon trap
4. Chemically heated catalyst
5. Exhaust gas ignition
6. Preheat burners
7. Cold-start spark retard or postmanifold combustion
8. Variable valve combustion chamber
9. Double-walled exhaust pipe

All of these approaches contain underfloor catalysts of various compositions. It has become clear that with the development of high-temperature close-coupled catalyst, this is the leading technology for most LEV, ULEV, and SULEV applications. The various candidate technologies are briefly described below, along with details of the close-coupled catalyst development.

#### 6.9.1 Close-Coupled Catalyst

The concept of using a catalyst near the engine manifold or in the vicinity of the vehicle firewall to reduce the heatup time has been published (Ball 1994; Bhasin et al. 1993; Summers et al. 1993). However, these were relatively low-temperature operations, and in any case, the maximum temperature was severely limited by the use of "overfueling" or "acceleration enrichment" to control the temperature (Wards 1993). The practice of "overfueling" or "acceleration enrichment" results in high HC and CO emissions and has come under pressure to be reduced or eliminated. Reducing this protection combined with an increase in the higher-speed driving habits in the United States and the existing autobahn driving habits increases the engine manifold discharge temperatures to around 1050°C, especially for 4- and 6-cylinder engines, thus changing the operating envelope of the close-coupled catalyst. In fact, a technology assessment published by CARB in 1994 showed the projected technologies for achieving the low emissions and close-coupled catalyst was not a viable option (CARB 1996). The dominant technology was the electrically heated catalyst. It is interesting that a cost study conducted in 1965 showed that the close-coupled approach was the least expensive solution; however, no suitable technology existed for the >100,000-mi durability requirements (Eade et al. 1995).

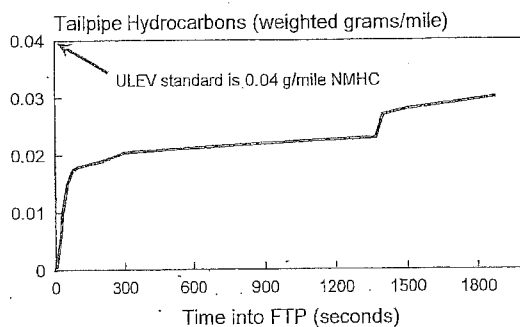


Figure 6.31 Close-coupled catalysts solve low-emission requirements. [Reprinted with permission, © 1995 Society of Automotive Engineers, Inc. (Heck et al. 1995).]

Catalyst manufacturers were once again exploring new carriers capable of retaining high surface areas and metal combinations that resist deactivation due to sintering after high-temperature exposure. A shift in the technology for close-coupled catalyst occurred when a close-coupled catalyst capable of sustained performance after 1050°C aging was developed and shown to give LEV and ULEV performance in combination with an underfloor catalyst (Hu and Heck 1995). The close-coupled catalyst was designed mainly for HC removal, while the underfloor catalyst removed the remaining CO and NO<sub>x</sub>. The concept inherent in this technology was to have lower CO oxidation activity for the close-coupled catalyst, thus eliminating severe over temperatures when high CO concentrations occur in the rich transient driving cycle. Subsequent studies on a 1.9-liter, 4-cylinder engine showed that a cascade designed close coupled catalyst could meet ULEV regulations as shown in Figure 6.31 (Heck et al. 1995). This shift in technology was significant enough such that when CARB conducted another survey for projected technologies in 1996 for achieving the low emissions, the close-coupled catalyst dominated the technologies, basically eliminating the electrically heated catalyst (CARB 1996).

With this benchmark set, other catalyst manufacturers worked on catalyst technologies capable of sustained operation and good HC lightoff after exposure to 1050°C. (Takada et al. 1996; Waltner et al. 1998; Williamson et al. 1999; Smalling et al. 1996) The characteristic of these close-coupled technologies is that Ce is removed. Ce is an excellent CO oxidation catalyst and also stores oxygen, which then can react with CO during the rich transient driving excursions. If the oxygen is stored on the catalyst during severe rich excursions (such as fuel enrichment or heavy accelerations), then the CO can react at the catalyst causing a localized exotherm, resulting in very high catalyst surface temperatures. As a rule, every percent of CO oxidized gives 90°C rise in temperature. This can cause severe sintering of the catalyst surface reducing the activity.

One study looked at the geometric effect of the close-coupled catalyst on both performance and lightoff. The cross sectional area and volume of the



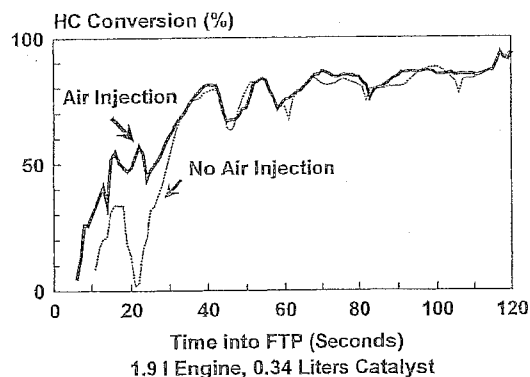


Figure 6.32 Oxygen in exhaust is key to cold start of close-coupled catalysts. [Reprinted with permission, © 1995 Society of Automotive Engineers, Inc. (Heck et al. 1995).]

close-coupled catalyst in the so-called "cascade design" was studied (Heck et al. 1995). It was found that the smaller cross-sectional close-coupled catalyst with less volume significantly improved the lightoff characteristics and could be combined with a larger cross-sectional catalyst with more volume to achieve ULEV-type emissions. This concept is now being practiced either as a cascade design or a small-volume stand alone close-coupled catalyst.

The early lightoff of the close-coupled catalyst can be accomplished by a number of methods related to the engine control technology during cold start. One of the initial methods was to control the ignition spark retard, which would allow unburned gases to escape the engine combustion chamber and continue to burn in the exhaust manifold, thus providing heat to the catalytic converter (Cahn and Zhu 1996). These engine control methods have become more sophisticated, as illustrated by the studies on actually controlling the degree of exothermic reactions in the exhaust manifold (Nishizawa et al. 1997; Marsh et al. 2000). In all of these control strategies it is important to have oxygen present in the exhaust gas for early catalyst lightoff as shown in Figure 6.32 (Heck et al. 1995).

#### 6.9.2 Hydrocarbon Traps

Another approach investigated was the hydrocarbon adsorption trap in which the cold-start HCs are adsorbed and retained, on an adsorbent, until the catalyst reaches the lightoff temperature (Figure 6.33). Hydrocarbon trap materials considered to date have been mainly various types of zeolite (silicalite, mordenite, Y-type, ZSM-5 and beta zeolite) with some studies on carbon-based material. Studies have been conducted to quantify the hydrocarbon species during the vehicle driving cycle (Takei et al. 1993; Kubo et al. 1993). For an inline hydrocarbon trap system to work, the hydrocarbons must be eluted from

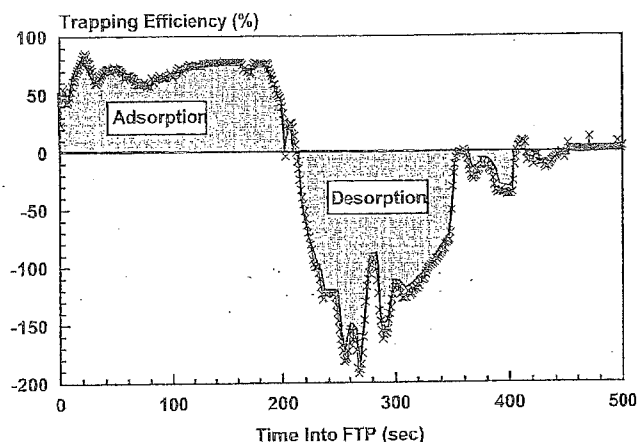


Figure 6.33 A hydrocarbon trap stores cold-start unburned hydrocarbons from vehicle.

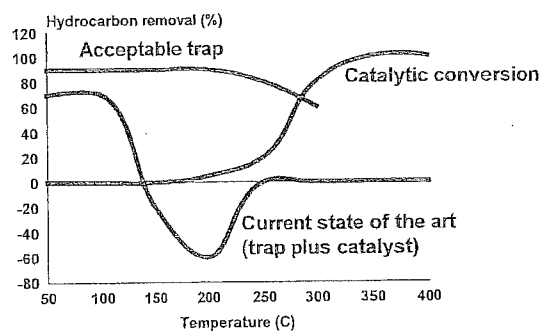


Figure 6.34 The lightoff of the catalyst is too late for cleanup of hydrocarbons released from hydrocarbon trap.

the trap at the exact time the underfloor catalyst reaches a reaction temperature  $> 250^{\circ}\text{C}$  as shown in Figure 6.34. These HCs are then desorbed and oxidized in the normal TWC catalyst. No hydrocarbon trap materials have been found capable of retaining HCs at this temperature. Consequently, hydrocarbons pass through the underfloor catalyst unreacted and then out the tailpipe.

However, some unique system designs have been proposed. A crossflow heat-exchanger-designed trap systems demonstrated a 70% reduction in the non-methane cold-start hydrocarbons during FTP cycle 1 (Hochmuth et al. 1993; Burk et al. 1995). Another trap design utilizes a cylinder with a central hole to allow passage of exhaust gas (Patil et al. 1996). This design contains a lightoff catalyst, the trap, and a downstream catalyst. Air is injected in the hole during cold start to divert the majority of exhaust flow to the trap in the cylin-

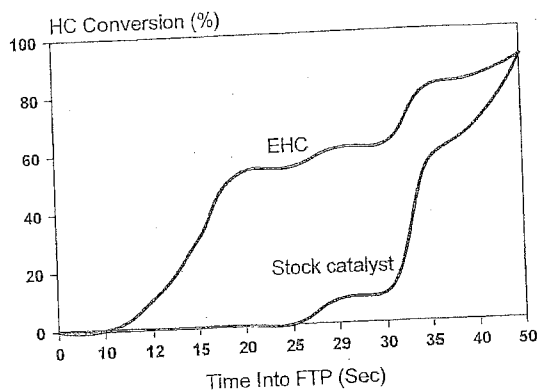


Figure 6.35 Electrical heated catalysts give low-emission performance.

der annulus. The small amount bypassed through the hole preheats the downstream catalyst. When the lightoff catalyst is functional and the downstream catalyst is up to the desired temperature, the air is turned off and the trap desorbs the HCs. These trap designs are interesting but have not been commercialized (Noda et al. 1997, 1998; Buhrmaster et al. 1997; Patil et al. 1998). There will be some commercial niche markets for trap systems used in combination with close-coupled catalyst or electrically heated catalysts. However, the trap will be designed for only a small portion of the cold start, in the first 10 s or so of the FTP, and not the entire cold start, as was the intention of these original studies.

### 6.9.3 Electrically Heated Catalyst (EHC)

Another approach to overcoming the cold temperatures during startup is to provide heat to the exhaust gas or the catalytic surface using resistive materials and a current/voltage source. Studies began prior to 1990 to develop an electrically heated monolith capable of providing in situ heat to the cold exhaust gas. If the electrically heated monolith is also catalyzed [an electrically heated catalyst (EHC)], then the preheat is directly applied to the catalyst surface. The EHC is placed in front of a small lightoff catalyst, which receives the preheated gas and thus provides a very efficient reaction during the cold-start period. Figure 6.35 shows the cold-start performance of an EHC. An underfloor catalyst that is much larger in volume supplies the reaction efficiency during the remainder of the driving cycle after the cold start.

Electrically heated monolithic catalysts are prepared in one of two ways (Socha and Thompson 1992; Gottberg et al. 1991; Abe et al. 1996; Kubsh and Brunson 1996; Shimasaki et al. 1997). One approach is to make a metal foil with the foils arranged to form an electrically resistive element. The catalytic washcoat is deposited on the metal. The element is attached to electrical con-

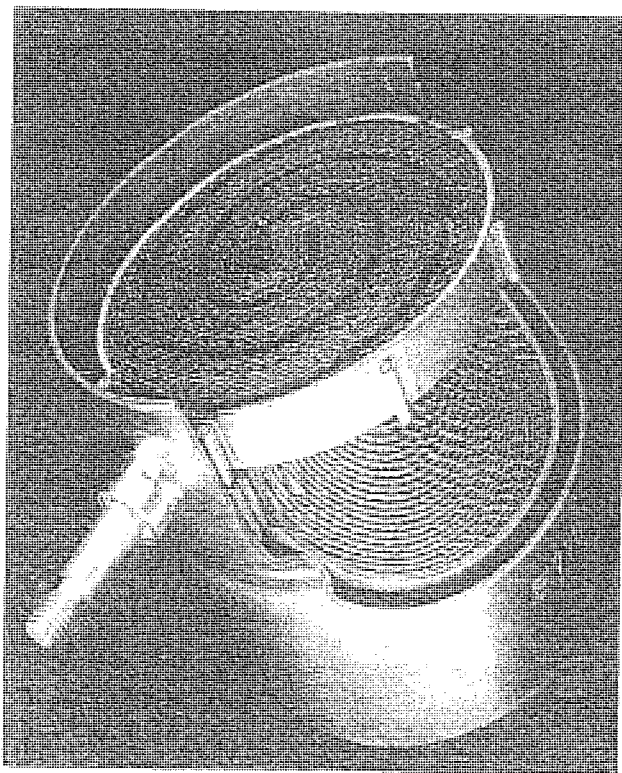


Figure 6.36 Cutaway of electrically heated catalyst. (Courtesy Emitec GmbH.)

nection points and can be heated quickly to the lightoff temperature of the catalyst (see Figure 6.36). Another approach is to make a monolith from extruded sintered metal and then deposit the catalytic washcoat. The base material in both cases is ferritic steel with varying amounts of Cr/Al/Fe with additives of rare earths. Substantial advances have been made in reducing the power requirements for EHCs, and studies have shown that the extra battery possibly can be eliminated, and the EHC can be powered off the vehicle alternator (Laing 1994). Electrically heated catalyst having low mileage has been shown to achieve ULEV; however, the durability to 100,000 mi is still an open issue (Kubsh and Brunson 1996). Actual in-use experience is being gained on larger vehicles, and these studies will give the needed "on the road" (on-road) experience with EHCs (Hanel et al. 1997).

#### 6.9.4 Noncatalytic Approaches

Three system design approaches have been proposed and studied in combination with catalysts to reduce the cold-start emissions. The preheat burner uses

the gasoline fuel in a small burner placed in front of the catalyst. The burner is turned on during cold start, and the heat generated warms up the catalyst so that the catalyst is hot when the cold exhaust from the manifold reaches the catalyst (Oser et al. 1994).

The exhaust gas igniter involves placing an ignition source (e.g., glow plug) in between two catalysts. During cold start, some of the cylinders of the engine are run rich to produce concentrations of CO and H<sub>2</sub> in the exhaust to make a flammable mixture. This is then ignited and heats the catalyst (Bade et al. 1996). The chemically heated catalyst uses highly reactive specie, usually H<sub>2</sub>, which is generated in a device onboard, the vehicle. Since this reacts at room temperature over the catalyst, the heat of reaction warms up the catalyst to react during cold start (Kamada et al. 1996).

These system approaches rapidly heat the catalyst during cold starts, resulting in low-emission operation; however, little is known of the system durability, and they are complex and expensive (Langren et al. 1994). None of these design options are presently being used in the new low-emission vehicles.

#### 6.10 MODERN TWC TECHNOLOGIES FOR THE 2000s

The modern TWC catalysts have taken the lead from the design of the Pd technology and are using layered catalyst with washcoat architectures to enhance the TWC reactions, and the high-temperature durability of the catalyst. The major components in a modern TWC are as follows:

- Active component—precious metal
- Oxygen storage component (OSC)
- Base metal oxide stabilizers
  - Precious metal
  - Alumina washcoat
  - Oxygen storage component
- Moderator or scavenger for H<sub>2</sub>S
- Layered structure
- Segregated washcoat

The Ce is now made as a Ce/Zr/X mixture (where X is a proprietary component), which stabilizes the OSC component for high-temperature operations. Ce is now added to the catalyst in various forms for a number of reasons:

- Oxygen storage
- Improved precious-metal dispersion
- Improved precious-metal reduction
- Catalyst for water–gas shift reaction, steam reforming, and NO reduction

More details on the beneficial effects of Zr on Ce began to be publicized in the 1996 timeframe. One study showed that 10–40% Ce in Zr was beneficial (Culley et al. 1996). Another study looked at the Ce/Zr ratio and the effect on performance after aging (Cuif et al. 1996). For a Pd catalyst, it was found that a 70/30  $\text{CeO}_2/\text{ZrO}_2$  solid solution showed superior redox properties compared to pure cerias or ceria with 10% zirconia as shown by oxygen storage (OSC) and temperature-programmed reduction (TPR) measurements (Cuif et al. 1998). Another study with Pd and Pt/Rh/Pd catalyst showed that the stabilization of the  $\text{Ce}/\text{ZrO}_2$  was bimodal and that the complex showed higher-surface-area maintenance at 10/90 wt% ratio and 90/10 wt% ratio (Yamada et al. 1997). This same study looked at stabilizing the Zr with different components of Al, Ba, Ca, Co, Cr, Cu, Mg, La, and Y. One study showed improved surface area stability by adding 15%  $\text{SiO}_2$  or 6%  $\text{La}_2\text{O}_3$  to a 30/70 (percent)  $\text{CeO}_2/\text{ZrO}_2$  system (Norman 1997). Strong enhancement of the activity of Ce rich  $(\text{Ce},\text{Zr})\text{O}_2$  solid solutions was shown when Pt was added (Cuif et al. 1997). The actual phase or structure of the Ce/Zr mixture has been the subject of some study and controversy (Egami et al. 1997). An unusual destabilization of the oxygen structure occurs at 450°C pointing at an ease of the structure to give up oxygen and generate defects. This intermediate solution approximates a solid solution at macroscopic levels and a physical mixture at the nanometer scale. It appears that the best Ce/Zr ratio is application-specific and depends on the automobile calibration, performance requirements, aging conditions, and catalyst formulation.

Also, the precious metals are segregated in the washcoat and are often prepared associated with a specific compound such as Rh/Ce/Zr and Pt/Al. In these catalyst designs, the deleterious interaction between Rh and Al is reduced. An illustration of the complex relationships between the precious-metal catalysts Pd and Rh and the Ce and Zr as well as the location in the bottom coat or top coat was done to show the interaction with fuel sulfur (Rabinowitz et al. 2001). The role of the ceria was complex.  $\text{NO}_x$  conversion was sharply improved by ceria, especially in combination with rhodium. However, under certain conditions, ceria, because of its ability to store and release sulfur, can be shown to increase the negative impact of sulfur. More details from the study are available in the original article, but this serves to illustrate the complex interactions present in today's scientifically designed automotive catalyst.

So, the major components of Ce, Al, and precious metals are stabilized in some sort for the modern TWC.

The effect of sulfur continues to affect the modern catalyst technologies. This effect has been quantified to be an actual selective poisoning effect and not a long-term effect on the catalyst performance (Bjordan et al. 1995). The sulfur affects mostly the lightoff characteristics of the TWC catalyst. As the sulfur is removed from the gasoline, the catalyst gradually regenerates and the performance is regained. The P and Zn in the lubricating continue to be an issue. One study looked into regenerating the TWC catalyst using chemical washing to remove the P and Zn deposits (Beck et al. 1995). The study concluded that the

P and Zn deposit could be removed using the chemical wash procedure, and once removed, the lightoff performance and conversion of the TWC catalyst improved. So, for the new low emissions standards, it will be important to reduce the fuel sulfur levels and oil blowby from the SI engine. Efforts should also be made to reduce the ZDP level of the lubricating oil.

### 6.11 TOWARD A ZERO-EMISSION STOICHIOMETRIC SPARK-IGNITED VEHICLE

This section could be entitled "putting it all together" or the "complete engineered system." During the later part of the twentieth century, the cooperation between the automobile manufacturers, the monolith suppliers, the exhaust system fabricators, the sensor manufacturers, and the catalyst manufacturers intensified so that a complete engineered system approach was taken to achieve the goal of a "zero-emission stoichiometric spark-ignited (SI) vehicle." With the advent of a durable close-coupled catalyst, many of the engine modifications to provide rapid heatup (e.g., spark retard on cold start) of the catalyst were now implemented. The ULEV performance requirement for a 4-cylinder vehicle, which may range from a hydrocarbon engine-out emissions of 1.5–2.0 g/mi, is around 98% hydrocarbon conversion. Of course, a SULEV vehicle is greater than 99% hydrocarbon conversion. As an aside, the tailpipe HC emissions from a SULEV vehicle may be less than 5 vppm HC, while the background level of ambient HCs is in the same range of 1–5 vppm, so the measurement of these low emission vehicles presents another challenge.

Because of these high emission reduction efficiencies and hence a requirement for more geometric surface area, monolith suppliers began to make higher cell density substrates approaching 1200 cpsi (Kikuchi et al. 1999; Gulati 1999). In addition, the exhaust piping was redesigned to minimize heat loss during the critical cold start with fabrication of the low heat capacity piping (Kishi et al. 1998a). Of course engine control must be better to minimize the perturbation effects on the TWC operation. To accomplish this, a new sensor was developed, based on the operating principles of the oxygen sensor but with more sophisticated design and electronics to give a gradual response curve to changes in A/F ratio or oxygen content in the engine exhaust. This universal exhaust gas sensor (UEGO) has the following operating characteristics as compared to the HEGO sensor as shown in Figure 6.37 (Anderson 1993, Bush et al. 1994). With this better control the operating window for the TWC is narrowed as shown in Figure 6.38. Of course the narrow operating window gives better overall HC, CO, and NO<sub>x</sub> conversion over the TWC.

Finally, demonstration of these ultra-low-emission systems became a reality (Sung et al. 1998; Kishi et al. 1998b, 1999; Nishizawa et al. 1997, 2000). LEV vehicles became common in the late 90s and ULEV vehicles were supplied to the California market in 1998. In 1999, a ZLEV (zero-level emission vehicle) vehicle was demonstrated after 100,000-mi aging (Kishi et al. 1999).

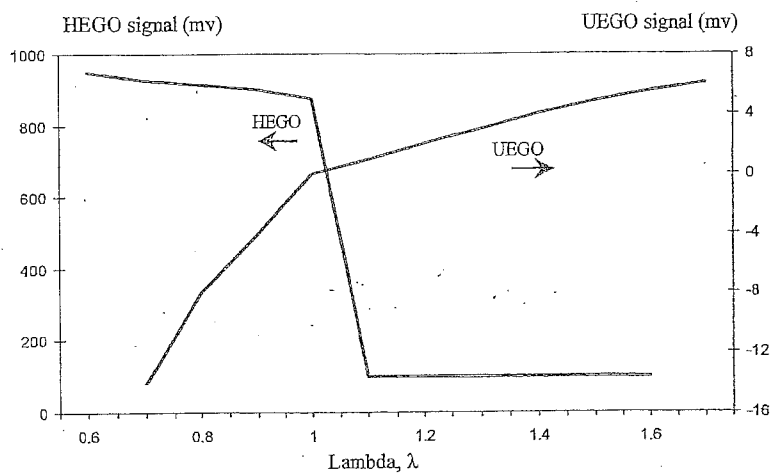


Figure 6.37 The response of the HEGO sensor is different from that of the UEGO sensor.

The following table represents the main characteristics for the Honda ULEV vehicle (Kishi et al. 1998b).

Engine Modifications	Exhaust Modifications
VTEC L4 with variable valve timing (VVT)	Low-heat-capacity manifold
ECU 32-bit microprocessor	UEGO sensor
Air-assist fuel injectors	Low-heat-capacity exhaust pipe
Precise A/F control with self-tuning regulation (STR)	Underfloor catalyst with Pd-only front on 600 cpsi
Electrically controlled exhaust gas recycle (EGR) valve	Secondary HEGO sensor
Individual cylinder A/F control	
Lean air/fuel cold start	

The key features regarding catalyst performance are the use of an engine designed as lean cold-start and fuel management to supply oxygen for the catalytic oxidation reactions and the reduction of heat loss during cold start. The new sensor for control is a universal exhaust gas sensor (UEGO sensor), which is a sensor whose response differs from that of the heated exhaust gas oxygen sensor (HEGO). So with the UEGO sensor the actual air:fuel ratio in the exhaust is known directly. The first underfloor catalyst is a 600-cpsi Pd catalyst designed for high-temperature operation, and the remaining underfloor catalyst accommodates emissions during normal operation. After 100,000 mi on a vehicle, the emissions measured were NMOG—0.03 g/mi; CO—0.35 g/mi; NO<sub>x</sub>—0.12 g/mi.



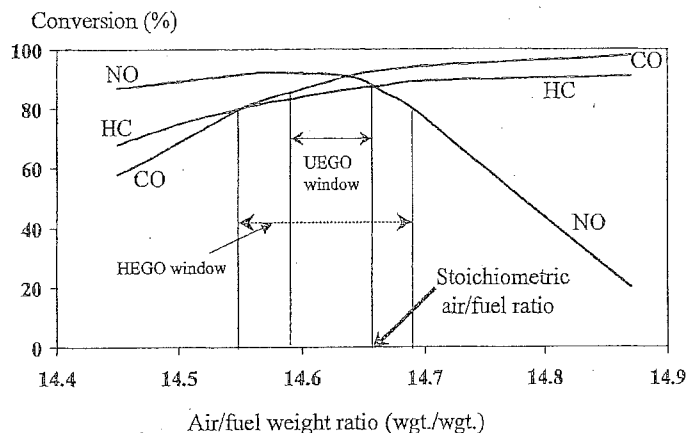


Figure 6.38 Example of how UEGO sensor control improves overall TWC performance.

The Honda so-called ZLEV vehicle is based on the same VTEC platform with additional controls for cold start for hydrocarbons and A/F control for  $\text{NO}_x$  (Kishi et al. 1999). The characteristics are summarized below:

Engine Modifications	Exhaust Modifications
VTEC L4 with VVT	Low-heat-capacity manifold
ECU 32-bit microprocessor	UEGO sensor
Improved atomization fuel injectors	Low-heat-capacity exhaust pipe
Precise A/F control STR	Pd close-coupled catalyst on 1200 cpsi
Individual cylinder A/F control	Underfloor catalysts TWC and HC
Ir and Pt sparkplugs	trap hybrid catalyst
Lean A/F cold start with spark retard	Two secondary HEGO sensors
Electrically controlled EGR valve	
Catalyst-condition-predicted control	

The engine utilizes spark retard during cold start to aid in catalyst heatup and lightoff. Also, the Pd close-coupled catalyst is 1200 cpsi followed by an underfloor catalyst system having a separate TWC and a trap-catalyst hybrid to manage the hydrocarbons during the first 10 s during cold start. After 100,000 mi on a vehicle, the emissions measured were NMOG— $<0.004$  g/mi; CO— $<0.17$  g/mi;  $\text{NO}_x$ — $<0.02$  g/mi.

Nissan has also demonstrated and now offers for sale the world's first certified partial zero-emission vehicles (PZEV) (Nishiwaza et al. 2000). This vehicle not only meets the SULEV tailpipe emissions but also has a zero evaporative emissions system and qualifies as a partial zero emission vehicle (PZEV). The

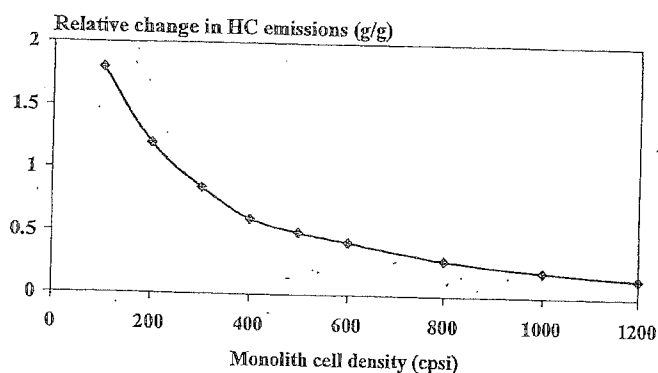


Figure 6.39 Increasing cell density required for low-emission vehicles. (Courtesy Emitec GmbH.)

engine emission control technology consists of a close-coupled catalyst followed by a series of trap-catalyst combinations to further reduce cold-start emissions. The Nissan Sentra CA vehicle has shown 150,000-mi durability and meets requirements for OBD (on board diagnostic) of the catalyst system (see Fisher et al. 1993 for explanation of OBD). This vehicle is also equipped with a PremAir catalyst-coated radiator, which removes ambient ozone (Hoke et al. 1996; Hoke et al. 1999; Greger et al. 1998). This catalytic device can be used to offset hydrocarbon tailpipe emissions or evaporative emissions. The PremAir technology will be covered in more detail in Chapter 15. This technology was first commercialized in December 1999 by Volvo, who utilized the concept for a "green" image on the V-70 model, and not for credits to offset tailpipe emissions. Nissan followed the same approach in 2000 by implementing PremAir catalyst on the radiator of the Sentra CA.

The excellent benefits of the increased cell density are shown in Figure 6.39. This study looked at the effect of changing the monolith cell density from 100 to 1200 cpsi and the effect on HC tailpipe emissions. The previous monolith technology was 400 cpsi, and the figures show the benefits of going to 600 up to 1200 cpsi. Approximately a 30% reduction is possible in going to 600 cpsi, while a 75% reduction is possible in going to 1200 cpsi. Another study was conducted using the European driving cycle, and this resulted in a similar conclusion as follows (Schmidt et al. 1999):

Cell Density (cpsi)	Wall Thickness (mils)	Emission Reduction (%)
400	6.5	Reference
400	4.3	12
600	3.6	35

These reductions in emissions were measured after the close-coupled catalyst of the different cell geometries.